Stony Brook University

Nitrogen Incorporation into Poly(diiododiacetylene) and Attempts Towards Synthesizing Push-Pull Diynes

A Thesis Presented

by

Gizem Eren

to

The Graduate School

in Partial Fulfillment of the

Requirements

for the Degree of

Master of Science

in

Chemistry

Stony Brook University

August 2014

Stony Brook University

The Graduate School

Gizem Eren

We, the thesis committee for the above candidate for the

Master of Science degree, hereby recommend

acceptance of this thesis.

Nancy S. Goroff – Dissertation Advisor
Associate Professor, Department of Chemistry

Kathlyn A. Parker - Chairperson of Defense
Professor, Department of Chemistry

Dale G. Drueckhammer-Third Member of Defense
Professor, Department of Chemistry

This thesis is accepted by the Graduate School

Charles Taber
Dean of the Graduate School

Abstract of the Thesis

Nitrogen Incorporation into Poly(diiododiacetylene) and Attempts Towards Synthesizing Push-Pull Diynes

by

Gizem Eren

Master of Science

in

Chemistry

Stony Brook University

2014

Cocrystallization is a method employed to orient diynes to achieve the appropriate parameters for topochemical polymerization. Using this technique, poly(diiododiacetylene) (PIDA) and 4-(Iodobuta-1,3-diyn-1-yl)benzoic acid are crystalized into their polymeric forms. The weak C-I bonds in PIDA have shown to break easily with Lewis bases like pyrrolidine and iodide. With the use of multiple deiodinating agents, PIDA has also shown to absorb the heteroatoms of present reducing agents in the final amorphous carbon product. Using sodium azide as a deiodinating agent, it has been theorized that nitrogen would incorporate into PIDA and produce a precursor to a carbon-nitride material based off of previous experiments.

Push-pull diynes are meant to narrow the band gap between a molecule's HOMO and LUMO. Efforts were made to modify the synthesis of the push-pull diyne, 4-(Iodobuta-1,3-diyn-

1-yl)benzoic acid. Previous work in the esterification of 4-bromobenzoic acid as well as the Sonogashira coupling reactions on t-butyl 4-bromobonzoate gave unsatisfactory yields. Different halogen moieties as well as different methods of esterification were explored.

Dedication Page

To those that were there during my most stressful moments, this is dedicated to my parents and loved ones.

Table of Contents

List of Figures

List of Schemes

List of Tables

List of Equations

List of Abbreviations

C12LG	4-O-lauryl-1,6-anhydroglucopyranose
C12mimCl	1-dodecyl-3-methylimidazolium chloride
C16mimCl	1-hexadecyl-3-methylimidazolium chloridel
CPC	Cetylpyridinium chloride
CTAB	1-hexadecyltrimethylammonium bromide
DMF	Dimethylformamide
DMSO	Dimethylsulfoxide
DTAB	Dodecyltrimethylammonium bromide
EDS	Energy-dispersive X-ray spectroscopy
FLG	Few layer graphenes
GE	General Electric
HEDM	High density energy materials
HMX	1,3,5,7-tetranitro-1,3,5,7-tetraazacylooctane
IL	Ionic liquids
IPA	Isophthalic acid
IR	Infrared Spectroscopy
ITAC12	Dodecylamine, 5,1-lauryl-4-carboxy-2-pyrrolidone
MeCN	Acetonitrile
MWCNT	Multiwalled carbon nanotubes
NMR	Nuclear magnetic resonance spectroscopy
PCBM	[6,6]-phenyl C_{61} butyric acid methyl ester
PCDA	Pentacosadiynoic acid
PCE	Power conversion efficiency
PDA	Polydiacetylene
PE-a-CTFE	Poly (ethylene-alt-chlorotrifluoroethylene) (PE-a-CTFE)
PIDA	Polydiiodoacetylene
PMM	Poly(methyl methacrylate)
RDX	(1,3,5-trinitro-1,3,5-triazacyclohexane
SDBS	Dodecylbenzenesulfonate
SDCI	Sodium dichloroisocyanurate
SDS	Sodium dodecyl sulfate
SEM	Scanning electron microscopy
SWCNT	Single walled carbon nanotubes
TEM	Transmission electron microscopy
THF	Tetrahydrofuran
TLC	Thin layer chromotography
TNT	(2,4,6-trinitrotoluene)
UV-Vis	Ultra violet visible spectroscopy

Chapter 1- Introduction

1.1 All-Carbon Materials

The discovery of new all-carbon materials has been of great interest for scientists since the application of diamond and graphite (**Figure 1.10**) in research and industry. Diamond and graphite are both found naturally within the environment; however in the past century, methods for synthesizing diamonds arose in order to meet the needs of industrial use. This synthetic diamond was first synthesized in 1954 by GE using carbon solvent/catalysts and research has expanded to include methods such as chemical vapor deposition.[1] Though diamond is important for its high thermal conductivity, hardness and high optical dispersion, other allotropes of carbon such as graphite and graphene, also possesses important properties.[2,2b-11]

Graphite is well known to many school children as the lead in their pencils. However, in 2004, Novoselov and Giem discovered that they could peel away layers from graphite and were able to sheer graphite to a single molecular sheet of honeycombed carbon, or graphene.[3] In addition, Novoselov and Giem found that these few-layer graphenes (FLG) were highly conductive, experiencing large sustainable currents, high ballistic transport (the transport of

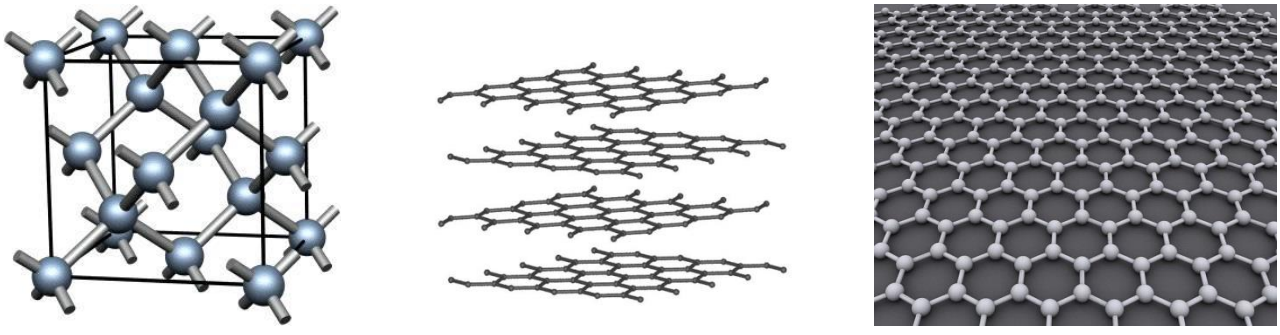

Diamond Graphite Graphene

Figure 1.1 Molecular structure of diamond (left), molecular structure of graphite (middle), and the molecular structure of a single layer of graphene (right).

electrons, without scattering caused by resistance of imperfections in materials) and a linear voltage.

Though graphitic carbon is important for thin films and conductivity research, the carbon allotrope, fullerene (**Figure 1.11**), used to be the highlight in solar cell research. Fullerenes are classified as hollow all-carbon material consisting of C_{60}, C_{70}, C_{76}, C_{82} and C_{84}, tubes and other numerous shapes. Fullerenes are used widely in photovoltaic applications; the fullerene C_{60} in particular, is used in electron-acceptor materials due to its ability to be reduced reversibly with up to six electrons.[4] C_{70} derived materials possess a higher absorption in the visible range, however it's much more expensive to synthesize compared to C_{60}.

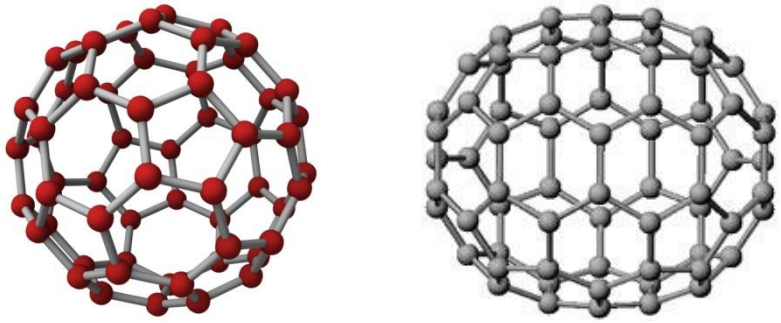

Figure 1.2 C_{60} (left) C_{70} (right)

In addition to their electrochemical importance, modified fullerenes have also shown to be effective anti-tumor agents. $Gd@C_{82}(OH)_{22}$ is a type of endohedral metallofullerenol molecule, has shown to induce tumor necrosis in lung, breast and liver cancer in mice.[5] Compared to other anti-tumor drugs such as cyclophosphamide and paclitaxel, $Gd@C_{82}(OH)_{22}$ showed a lower toxicity. In addition, Meng et. al., found that there was no significant difference observed in body weight between the control group and those treated with the fullerene

derivative. This demonstrates that the fullerene derivative does not trigger the weight loss in subjects, which is a side effect of cyclophosphamide and paclitaxel.

However, fullerenes are best known for their electrochemical properties and their applications in solar cells; more specifically they dominate in n-type materials. Fullerenes are used mostly in bulk heterojunction solar cells due to their low lying lowest unococcupied molecular orbital energy levels, fast photo-induced electron-transfer and high intrinsic electron mobility.[6] Used mostly in bulk heterojuntion solar cells, fullerenes offer great promise as the electron accepting component with power conversion efficiencies (PCE) close to 6%.[7] In fact a relatively high power conversion efficiency was reported to [6,6]-phenyl C_{61} butyric acid methyl ester (PCBM) (**Figure 1.12**) at 4-5%. However, Scharber et al., theorized that PCBM could possibly have a 10% PCE combined with an acceptor molecule.[8] The effectiveness of fullerene derivatives in both biological and electrochemical research has led to a broad range of scientific study on this topic.

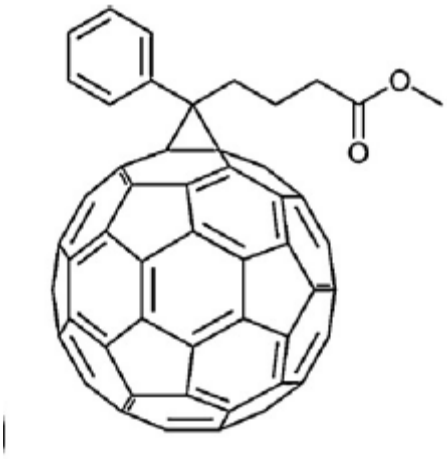

Figure 1.3 [6,6]-phenyl C61 butyric acid methyl ester (PCBM) Copyright [8]

Since the 1980s, the synthesis of carbon nanotubes has become a prominent interest of scientists for their catalytic, semiconducting and thermal conductivity.[9] Carbon nanotube research revolves around single walled carbon nanotubes (SWCNT) or multi walled carbon nanotubes (MWCNT) (**Figure 1.13**) and functionalized carbon nanotubes.

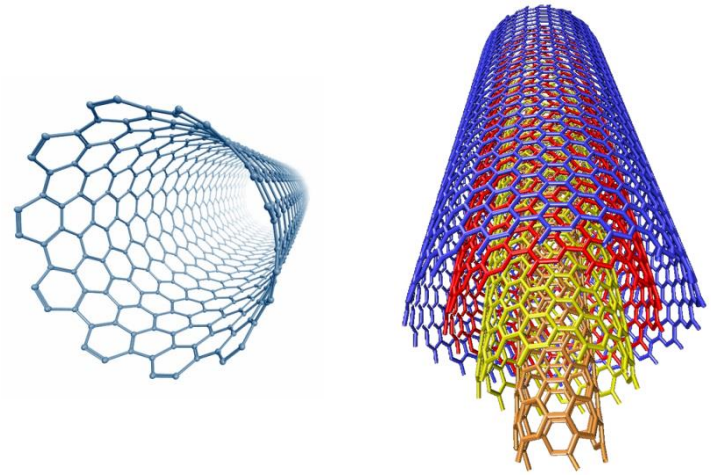

Figure 1.4 Single Walled Carbon Nanotube (left) and Multiwalled Carbon Nanotube (right)

Due to their hollow structure and large specific surface area, carbon nanotubes are ideal candidates for adsorption of toxic contaminants from industrial waste. The most concerning of such industrial wastes are organic dyes discharged from textile, leather, cosmetic etc. industries which have high levels of biotoxicity in humans; dyes such as Sudan red I, II, III and VI have high toxicity and are carcinogenic at low concentrations.[10] Methylene blue is an organic dye commonly used in medicine as an antimalarial drug but it can be toxic at high doses. Using methylene blue as a model dye, Ai and Jiang prepared self-assembling graphene and nanotube hybrid materials that showed a 97% and 91% removal of methylene blue with concentrations of dye at 10 and 30 mg L respectively.[11]

1.2 Functionalized Carbon Materials & Carbon Rich Materials

Though applied to numerous areas of research as discussed in the previous section, carbon materials can be modified to broaden their utility. Adding functionalities to carbon rich materials could increase their solubility in organic solvents, increase surface wettability in carbon electrodes, or create catalytic activity.

When functionalizing carbon materials, doping materials with heteroatoms has shown to enhance the electrochemical performance of carbon electrodes which, on their own, only have a moderate capacity compared with metal oxides and conducting polymers.[12] Nitrogen containing functionalities, in particular, exhibit electron-donor properties and can increase the conductivity of electrodes. Wang et al., recently utilized polyaniline as a nitrogen and carbon source in order to obtain an n-doped carbon network. By adding polyaniline to a suspension of SiO_2, carbonizing and activating with KOH at 850^{o}C, they were able to acquire a high specific area (1676 m^2g^{-1}), large pore volume (2.13cm^3g^{-1}) which is favorable for rapid mass transfer and ion diffusion which in turn improves the performance of supercapacitors. There was also a high nitrogen concentration (5.7wt%) which Wang et. al., speculate as having improved the surface wettability of the carbon eletrode. These N-doped carbon materials show great promise in energy storage devices and are an increasingly more popular area of study.

Like carbon's allotropes, carbon nanotubes are exceptionally versatile. Metal based catalysts pose disadvantages in their poor durability, high cost and environmental toxicity. N-doped graphene nanotubes are a safer and more efficient alternative in that they have long term stability and a good tolerance against CO poisoning, problems present in Pt-based electrodes.[13] Cheng et.al., synthesized an n-doped graphene/carbon nanotube nanocomposite at low

temperatures (180^{o}C) using graphene oxide, oxidized multi-walled carbon nanotubes and ammonia as a precursor.[14] Though far from practical applications in fuel cells, n-doped graphene/carbon nanotubes are a promising electro-catalyst for use in the search for renewable energy.

1.3 Nitrogen-Rich Materials

Nitrogen-rich compounds are highly energetic materials with high densities and hardness. Compounds rich in nitrogen possess high heats of formations and combustions; these characteristics make them good candidates in propellants as they are capable of moving pistons and turbines and any device that requires high rates of energy transfer.[15,16] Military based explosives are mostly all nitrogen based compounds: HMX (1,3,5,7-tetranitro-1,3,5,7-tetraazacylooctane), RDX (1,3,5-trinitro-1,3,5-triazacyclohexane), TNT (2,4,6-trinitrotoluene), and the well-known nitroglycerine.[16] These highly energetic compounds are also environmentally friendly; their primary decomposition product is molecular N_2. However, these compounds are shock sensitive, and recent research has focused on creating new high density energy materials (HEDM) that are insensitive to shock, heat, friction, and are generally stable compounds.[15-19]

Traditionally, high energy materials are thought to derive their energy from the oxidation of the carbon backbone; a dense molecule can possesses enough oxygen to oxidize the carbon backbone and hydrogen atoms into gaseous CO, CO_2, or H_2O.[17] However, Chavez et al. stated that high nitrogen compounds derive their energy from high positive heats of formation as opposed to the oxidization of the carbon backbone. Their previous work with azo-1,2,4,5-tetrazines found that there was a 327 kJ mol $^{-1}$of energy gained in the formation of an azo linkage between heterocyclic rings of their molecule presented in (**Scheme 1.1**).[18] Chavez et al. extrapolated that 1, 3'-azobis(6-amino-1,2,4,5-tetrazine) (**Figure 1.5)** would have a higher heat

of formation due to the tetrazine ring. Once synthesized and purified, 1,3'-azobis(6-amino-1,2,4,5-tetrazine) was stable at 252°C, and the heat of formation was measured to be +862 kJ mol^{-1}.[18]

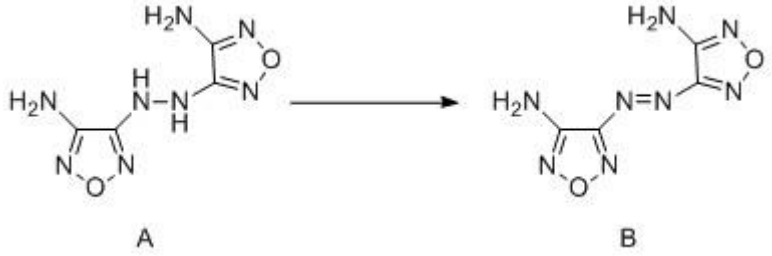

Scheme 1.1 For molecule A ΔH_f = 209 kJ mol^{-1} and for molecule B, ΔH_f=536 kJ mol^{-1}.[18]

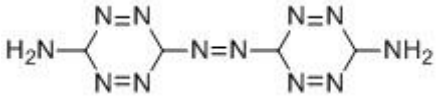

Figure 1.5 1,3'-Azobis(6-amino-1,2,4,5-tetrazine)

Similarly, tetrazoles have been also been at the forefront of high-energy materials research. As stated previously, the azo linkage between the cyclic structure increases the heat of formation as well as desensitizes the material.[19] Li et al., successfully synthesized 1-1'-azobis-1,2,3-triazole by the treatment of 1-amino-1,2,3-triazole with sodium dichloroisocyanurate (SDCI) at low temperature for 30 minutes (**Scheme 1.2**).[19]

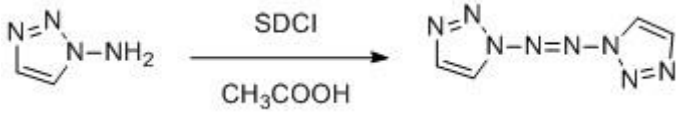

Scheme 1.2 Treatment of 1-amino-1,2,3-triazole with sodium dichloroisocyanurate to produce 1-1'-azobis-1,2,3-triazole with a 78% yield.[19]

The decomposition temperature of the tetrazole was determined to be 193.8 °C, remarkably high for an 8-nitrogen compound. In addition, the heat of formation of the tetrazole was determined to be +962 kJ/mol and it surprisingly underwent a reversible chromatic shift when subjected to

irradiation. These high density nitrogen molecules prove their decomposition yields large quantities of energy.

1.4 Carbon Nitrides

The growth of industry demands stronger, lighter and overall better materials for use in cutting, coatings, etc., in any and all aspects of manufacturing. Over 25 years ago silicon nitride (Si_3N_4) was investigated due to its lightweight, low inertia components with excellent strength-to-weight ratios. In 1989, Liu and Cohen determined the first-principle pseudopotential study of the structural and electronic properties of β-Si_3N_4.[20] In conjunction with β-Si_3N_4,the investigation on C_3N_4 was spurred by previous research by Cohen. Cohen's previous bulk moduli work of tetrahedral solids with short bond lengths focused on conceiving new low compressible solids which led to the investigation of C_3N_4.[21] Bulk modulus is related to the bond length between atoms; the C-C bond length in diamond is 1.54Å whereas a C-N bond length in typical organic molecules is 1.47Å. With this shorter bond length between atoms, it is believed that tetrahedral structures of C_3N_4 could possibly have the same bulk moduli comparable to diamond, if not larger.[21] Liu and Cohen calculated the bulk moduli for the hypothetical compound of C_3N_4 and it was comparable to diamond (4.27 Mbars to 4.43 Mbars respectively) and that the cohesive energy was so large (81.5 eV/cell) that it would exist in a metastable state. Ever since their calculations, scientists have attempted to prepare the crystalline phase β-C_3N_4 but have been unable to isolate a pure compound.[22-26,28] Instead efforts have been made to create γ-C_3N_4, graphitic C_3N_4 and an amorphous material containing all phases of C_3N_4.

Obtaining carbon nitride networks, either graphitic or crystalline, is difficult and requires high heats and/or pressures. The results are generally in the metastable state; amorphous carbon nitride materials with traces of the desired phases. A purely crystalline form of C_3N_4 has not

been achieved and therefore not characterized and much of the data on the crystalline phases obtained is ambiguous.[22-26] Nevertheless, there are multiple phases of C_3N_4 predicted. The α and β phases are thought to be tetrahedrally coodinated and differ only in their stacking. The α phase is the AB stacking of a β-C_3N_4 layer.[22] Then there is the predicted cubic C_3N_4 arrangement, or the γ-C_3N_4 which is the only phase to possess C-C and N-N bonds. Regardless of the multitude of predictions, synthesizing a pure phase of any C_3N_4 material has not been achieved and is still under investigation.

One of the few first steps taken for bulk production of C_3N_4 was by Montigaud et al., who used a condensation of melamine and cyanuric chloride in order to obtain the graphitic type carbon nitride (**Scheme 1.3**). [23]

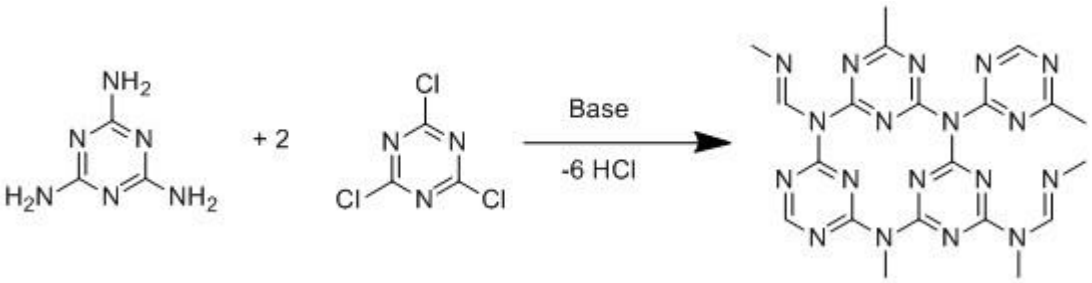

Scheme 1.3 Condensation of melamine and cyanuric chloride.[23]

However, the solid that Montiaguad et al., obtained was unstable and though it presented a graphitic like structure it possessed an undesirable number of hydrogens which should not be present at all in a pure C_3N_4 material. The presence of hydrogens, however, was attributed to the formation of NH_3 and thus the condensation of melamine and cyanuric acid was incomplete. Montiaguad et. al., also attempted the solvothermal treatment of melamine with an azide source, hydrazine. This second route produced an amorphous mixture of graphitic nature. The IR analysis of the product showed a stretch at 3200 cm^{-1}, corresponding to the N-H stretch, a stretch at 1310 cm^{-1} which corresponds to the C(sp^2)-N stretching mode and 1610 cm^{-1} which

corresponds to C(sp^2)=N stretch, the stretching modes of graphitic like structures. But most of the analysis not a clear pathway to forming carbon nitride networks, nor was any of the material produced a well-developed material.

Semencha et. al., prepared a carbon nitride compound using two different methods; the thermal decomposition of sodium and potassium thiocynate at 450 ^{o}C and the reaction of liquid ammonia with carbon tetrachloride.[24] Using X-ray powder diffraction, IR spectroscopy, mass spectroscopy and electron microscopy, Samencha et al., found peak frequencies at 1626 and 1050 cm^{-1} from the brown solid they obtained, attributing them to the C=N and C-N bonds. However, in both reactions they also found nitrile peaks at 2250 cm^{-1}, the nitrogen to hydrogen ratio was not reported, and again, the signal to noise in most of the characterizations leaves the results open to scrutiny.

Attempting to veer away from traditional methods, Fahym et. al., used a mechano-chemical synthesis and produced what could be a small amount of β-C_3N_4. Graphitic carbon was ball milled and a nitrogen sources was added by the use of either liquid nitrogen or liquid ammonia to generate amorphous carbon material with trace amounts of β-C_3N_4 detected via x-ray powder diffraction.[25] The diffraction data obtained by Fahmy et al. suggests that there are trace amounts of nanocrystalline β-C3N4 present in the sample where liquid ammonia was present. Most of the characterization techniques, however, have such a large background signal which essentially becomes the usual problem with characterizing C_3N_4 products.

Thermolysis or thermal decomposition of starting materials has generally been the trend with a large portion of attempts to produce C_3N_4. Focusing on decomposing high nitrogen azides, Edward G. Gillian reported a nitrogen rich precursor, (C_3N_3)-$(N_3)_3$, and studied its decomposition at T > 200 ^{o}C and varying pressures at 1 and 6 atm under a nitrogen flow. What

resulted was graphitic nanoparticles and N_2 gas.[26] Elemental analyses were taken of the varying products. The solid state ^{13}C NMR showed peaks at 158 and 156 ppm which are indicative of sp^2-bonded carbon. The IR spectra displayed peaks consistent with conjugated C=N and C=C (1600 – 1700 cm^{-1}), aromatic rings (1450 – 1600 cm^{-1}), N=N bonds (1440 cm^{-1}), and 1,3,5-substituted rings (810-950 cm^{-1}). Elemental analysis (wt %) showed a large nitrogen content in the carbon material; C (34.45), N (61.78), H (<0.05), and O (2.34). It was determined that the film and powder obtained was C_3N_4 and C_3N_5. Using higher pressures and flushing with excess nitrogen increased the nitrogen content. However, there were small percentages of hydrogen present that were attributed to tying up reactive bonds. Possible decomposition pathways are illustrated in **Scheme 1.41**.[26] Most of Gillian's assumptions are based on IR spectra, UV-vis spectra and ^{13}C chemical shifts; both the IR and UV-vis showed intact triazine (sp^2) rings structures and very small cyanide or carbodiimide absorptions indicated that there wasn't a large number of side reactions. Experimentally, Gillian achieved a disordered product with no clear crystalline structure.

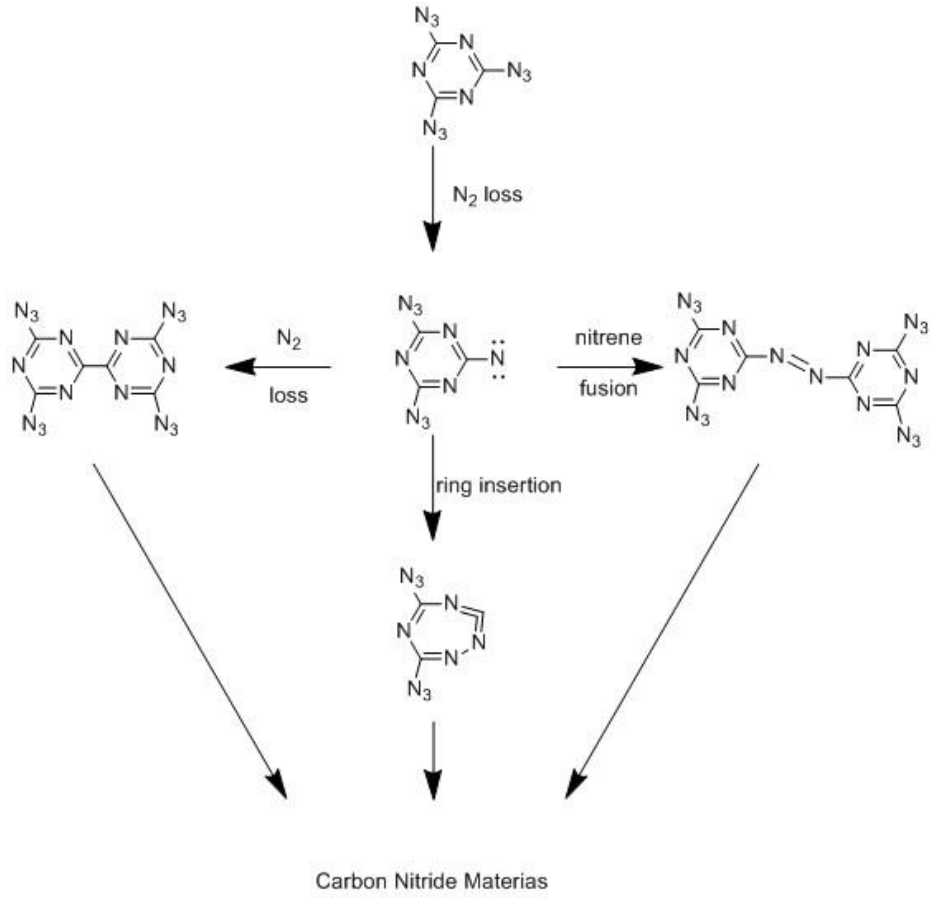

Scheme 1.4 Decomposition pathways of (C_3N_3)-$(N_3)_3$**.**

In the past year a purely graphitic C_3N_4 material with no amorphous material and a clear graphitic structure has been successfully synthesized. Algara-Siller et. al., reported the effective synthesis of not only g-C_3N_4 but a thin film down to approximately three atomic layers.[27] The monomer, dicyandiamide was heated to 600^{o}C in a eutectic mixture of LiBr and KBr. The product formed is a continuous film of triazine based graphitic carbon nitride. High resolution TEM images show a hexagonal 2D honeycomb arrangement with a unit cell of 2.6Å shown below in **Figure 1.6**.In addition to its successful production, the purely graphitic carbon nitride is deduced to have a bandgap similar to semiconductors such as Si, GaAs and GaP and thus has potential to be a post-silicone semiconductor.

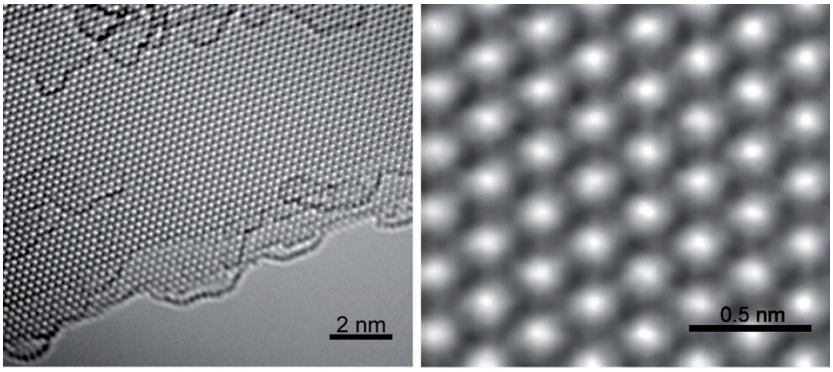

Figure 1.6 TEM image of Triazine based graphitic carbon nitride showing a hexagonal 2D arrangement with the three coordinated nitrogen atoms in the bright areas (right). Copyright [27]

In addition to using azide and graphitic precursors to obtain carbon nitrides, using small molecules rich in nitrogen is not uncommon when trying to obtain new carbon nitride materials, yet diacetylenes have rarely been used as a nitrogen rich precursor. In fact, one of the few in the past 35 years using diacetylenes as a route to N-doped graphitic carbons was Fahsi.[28] Two diacetylene precursors were chosen, 1,6-bis(1-imidazolyl)-2,4-hexadiyne monohydrate and 1,6-bis(1-benzimidazolyl)-2,4-hedadiyne (**Figure 1.7**).

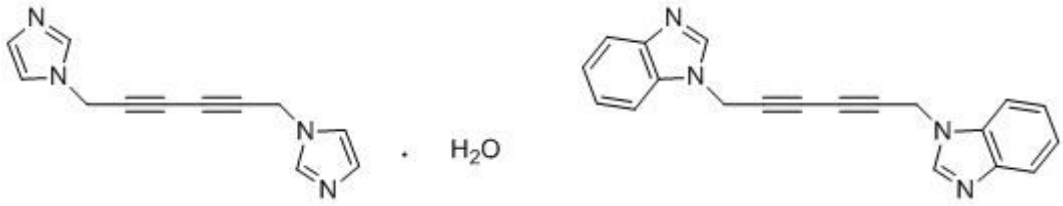

Figure 1.7 1,6-bis(1-imidazolyl)-2,4-hexadiyne monohydrate (left) and 1,6-bis(1-benzimidazolyl)-2,4-hedadiyne (right)

The diacetylenes were subject to pyrolysis at varying temperatures from 110 to 1100 ^{o}C. The two diacetylenes were found to have a highly exothermic phenomenon at low temperature that corresponds to the transformation of these two monomers into polyaromatic structures. The graphitic-carbon like materials obtained also had nitrogen contents of 7.4% and 8.4%. The nitrogen content, though not exceptionally high, is the only reported procedure utilizing

diacetylenes as precursors. Though in its early stages, using diacetylenes as precursors and subjecting them to decomposition with a nitrogen source present could lead to new methods of obtaining carbon nitride materials without having to undergo harsh conditions previously stated. The use of milder conditions could benefit future research in order to save time and cost in the consumption of material and labor.

Chapter 2- Polydiacetylenes and Poly(diiododiacetylene)

2.1 Polydiacetylenes

Polydiacetylenes (PDAs) have become large forerunners in organic research and material due to their optical, physical and electronic properties. The polymer backbones of PDAs possess alternating eyn-yne groupings that are responsible for their blue to red chromatic shifts (**Figure 2.1**) and play a large role in bio- and chemo- sensing.[1]

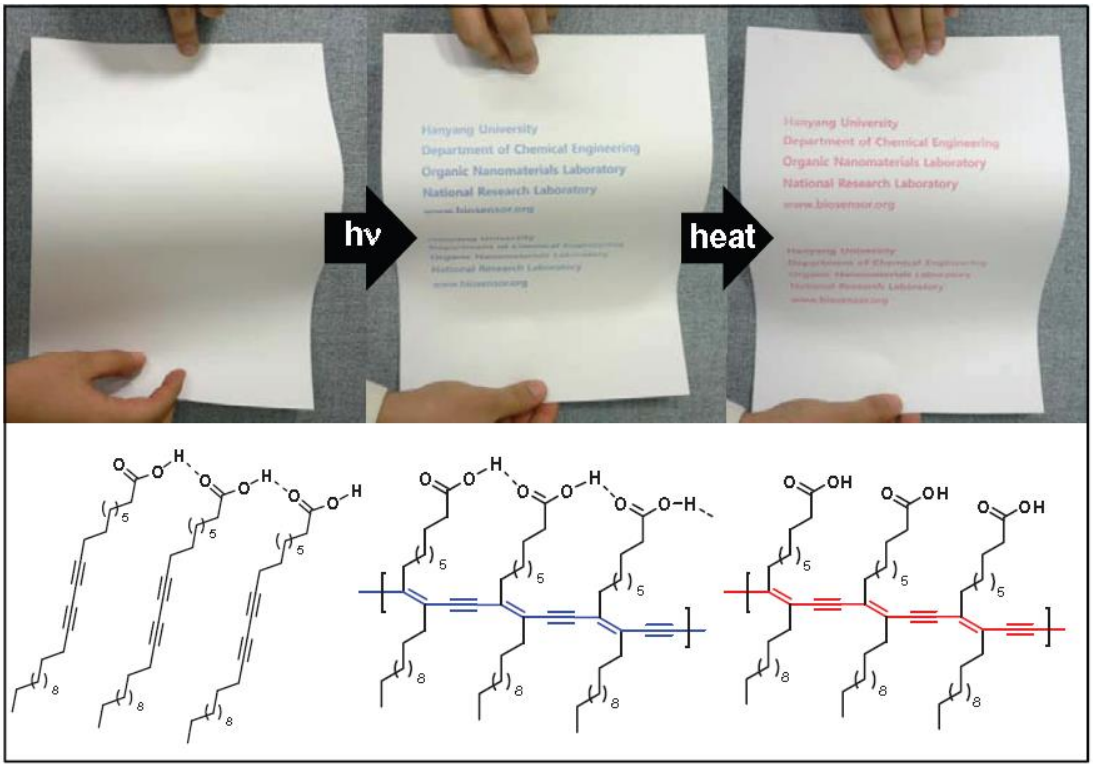

Figure 2.1 The blue to red chromatic shift illustrated in the use of inkjet printing. Reproduced from [3] with permission from The Royal Society of Chemistry.

This red to blue chromatic shift (an absorption peak from 640 nm to 500 nm) is attributed to the electron delocalization and results in shorter electronic delocalization lengths.[29] In addition, the chromatic properties of PDAs were linked to the conformation of the polymer chain.[30]

PDA monomers are generally easy to polymerize through UV or γ-light irradiation and can be polymerized into one, two or three dimensional structures.[31] One-dimensional structures of PDAs are typically single chained diacetylene molecules that usually form a nanofiberous or nanotubular structure.[1,2] Lee et al., synthesized a fluorogenic PDA polymer from isophthalic acid (IPA)- derived diacetylene (F**igure 2.2**) and found that it self-assembled into fibers.[32] When UV irradiated, the monomer formed blue micro-wires that are associated with the conjugated polymer.

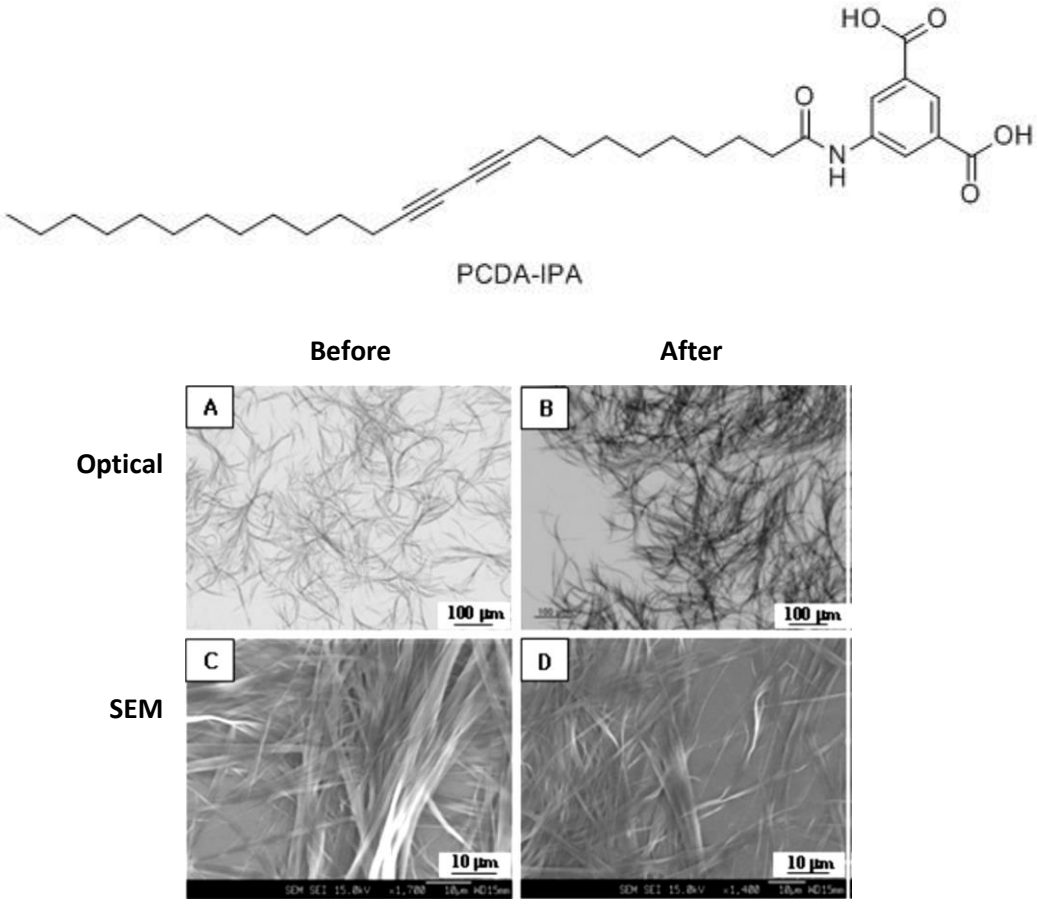

Figure 2.2 (Top) Isopthalic acid (IPA) derived diacetylene. (Bottom) Optical (A and B) and SEM (C and D) images of PCDA-IPA ribbons before (A and C) and after (B and D) UV irradiation (254 nm, 1mW/cm3, 1 min). Copyright [3]

When a glass slide with a drop of suspension of the polymer was heated to 100^{o}C, there was a blue to red chromatic shift, characteristic of PDAs and this blue to red chromatic shift characterizes the 2D structure of PDAs.[1-4] Yoon et al., prepared multiple 10,12-Pentacosadiynoic acid (PCDA)-based (**Figure 2.3**) diacetylene monomers that could be

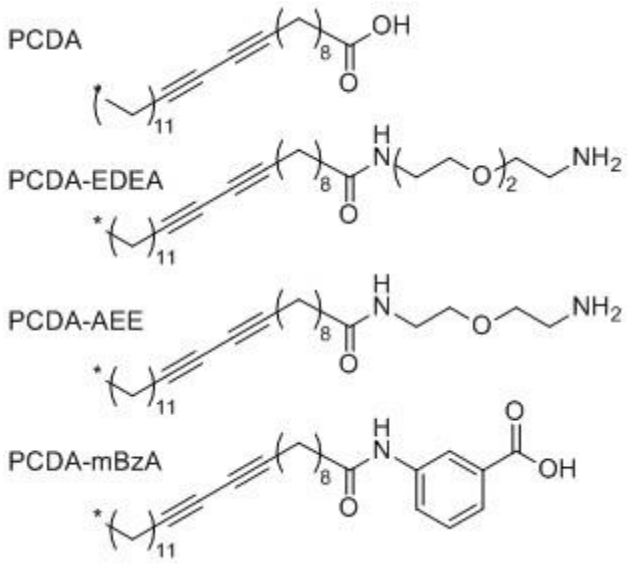

Figure 2.3 PCDA Monomers

combined with commercially available ionic (SDS, DTAB) and nonionic (Brij 72, Brij 78, Brij S100) surfactants to make ink for inkjet printers.[33] The PCDA-mBzA-Brij 78 suspension was used to create bank notes that would prove to combat counterfeiting; by irradiating the banknote, Yoon et al., observed a blue-to-red color change (**Figure 2.4)**. The ink suspensions are all stable for prolonged periods of time if kept cold (4^{o}C).

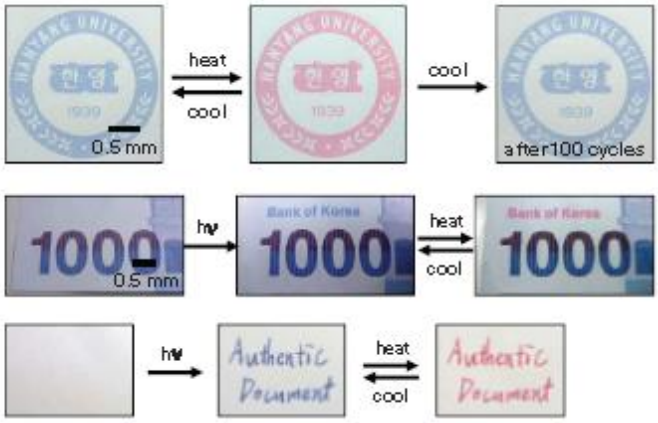

Figure 2.4 The use of PDA's in printing in order to combat counterfeit currency. Initially invisible, the ink is irradiated to bring about the blue shift and the PDA can be heated reversibly

Fully utilizing the potential of PDAs and implementing them into commercial use, especially in areas of sensing, requires the generation of PDA films in order to implement them into sensing devices. The most commonly used technique for thin film deposition is the Langmuir technique, in which PDA monomers are deposited onto a water surface, compressed, and then polymerized before deposition onto a substrate.[2] In addition to the Langmuir method, spin coating of PDA monomers is also a method utilized in film preparation. Kootery et. al., studied the color change of two spin coated monomers, 10,12-tricosadiynoic acid or 10,12-tricosadiynoic acid/10,12-tricosadiyn amine mixture, by heat and the use of different analytes in order to analyze structural, photophysical and sensing properties with the hopes of implementing into chemo- and biosensing materials.[34] PDA monomers were deposited onto poly(methyl methacrylate) (PMM) via spin casting and a broad range of analyst varying in structure, charge and functional groups were added atop the polymerized films; [1-hexadecyltrimethylammonium bromide (CTAB) , and cetylpyridinium chloride (CPC)], ionic liquids (ILs) [1-dodecyl-3-methylimidazolium chloride (C12mimCl) , and 1-hexadecyl-3-methylimidazolium chloride (C16mimCl)], weak acid/base surfactants [dodecylamine, 5,1-lauryl-4-carboxy-2-pyrrolidone (ITAC12)], non-ionic surfactants [4-O-lauryl-1,6-anhydroglucopyranose (C12LG) , and Triton

X-100], and anionic surfactants [sodium dodecyl sulfate (SDS) and sodium dodecylbenzenesulfonate (SDBS) (**Figure 2.5**). The most striking transition was experienced by the positively charged bulky head groups which gave a blue to yellow/orange transition. These specific color transitions with the use of different amphiphilic analytes could be of good utilization for the development of biological and chemical sensing applications.

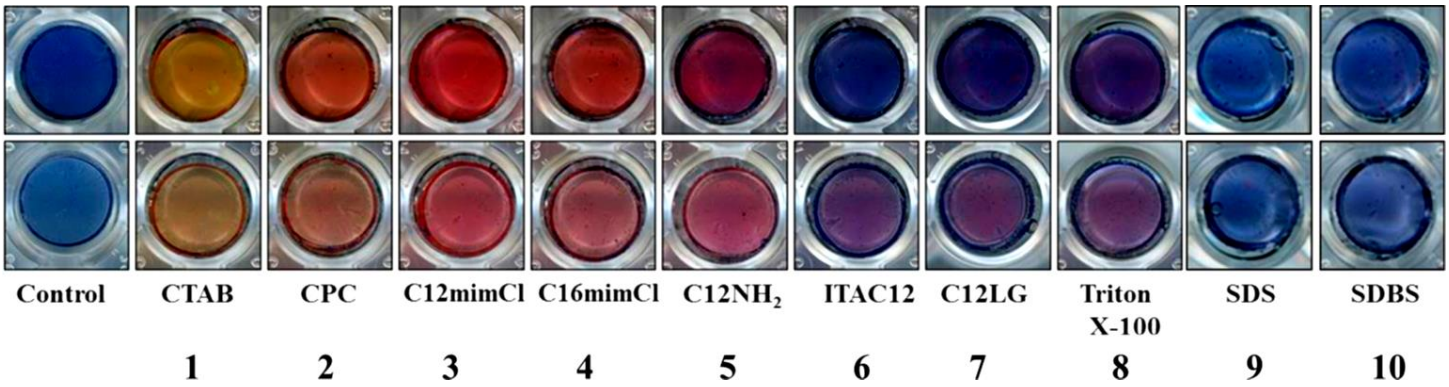

Figure 2.5 Color changes induced by analyst. Scanned images of PDA/PMMA (top row), and PDA-NH2/PDA/PMMA (bottom row), after addition of the analyts (concentrations 1 mM). Images were recorded after 40 min incubation 31-hexadecyltrimethylammonium bromide (CTAB) 1, and cetylpyridinium chloride (CPC) 2], ionic liquids (ILs) [1-dodecyl-3-methylimidazolium chloride (C12mimCl) 3, and 1-hexadecyl-3-methylimidazolium chloride (C16mimCl) 4], weak acid/base surfactants [dodecylamine, 5,1-lauryl-4-carboxy-2-pyrrolidone (ITAC12) 6], non-ionic surfactants [4-O-lauryl-1,6-anhydroglucopyranose (C12LG) 7, and Triton X-100 8], and anionic surfactants [sodium dodecyl sulfate (SDS) 9 and sodium dodecylbenzenesulfonate (SDBS) 10

However, the more interesting 3D PDAs contain a larger surface area and multipoint interaction sites for sensor applications. Nevertheless, most of PDA polymer properties depend on the functional groups on the monomers used.

2.2 Polydiiododiacetylene (PIDA)

In 2008 Sun et al., synthesized smallest PDA to date: Polydiiododiacetylene.[35] Using a host molecule to properly align the diiiodobutadiyne (**1**) monomer, Lauher and Fowler were able to arrange monomers through intermolecular interactions that fit into the parameters calculated by Wegner and optimized by Baughman (**Figure 2.6**).[36]

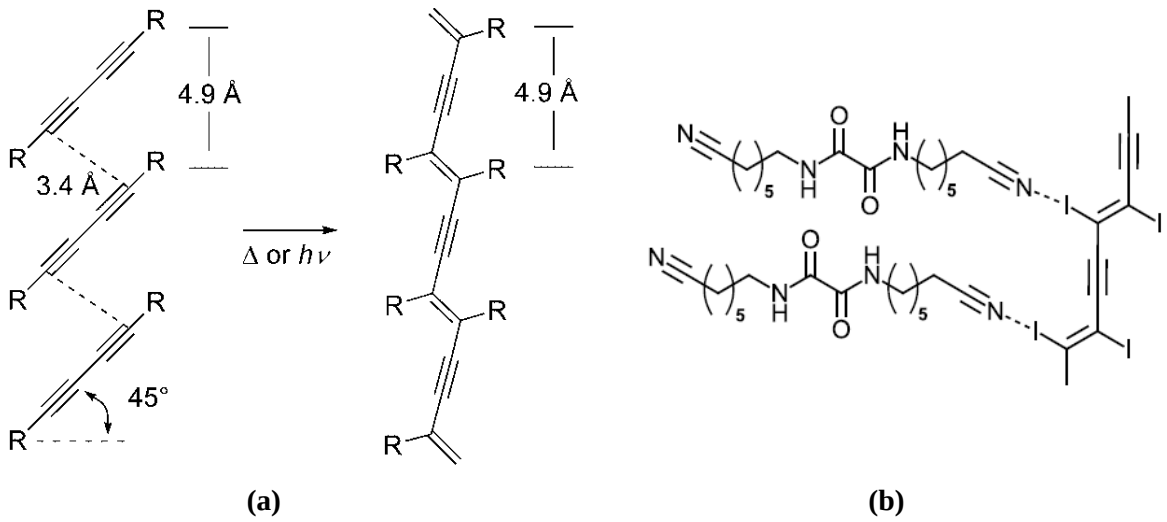

(a) **(b)**

Figure 2.6 (a) Ideal paramaters calculated by Wegner and optimized by Baughman.. (b) Cocrystal formation and 1,4 –topochemical polymerization of PIDA with an oxalamide host. Reprinted with permission from [9] Copyright (2013) American Chemical Society

Using the host-guest strategy implemented by Lauher and Fowler, the monomer, diiodobutadiyne **1**, was cocrystallized with numerous host molecules (**Figure 2.7**).[37] A large portion of these host molecules are oxalamides (Host **2a** & **2b**) that can halogen bond to the iodine molecule in diiodobutadiyne and bring it within the appropriate parameters for polymerization. The Lewis acidic halogen atoms in **1** create a noncovalent interaction that provides an order required for a three-dimensional crystal structure.[38]

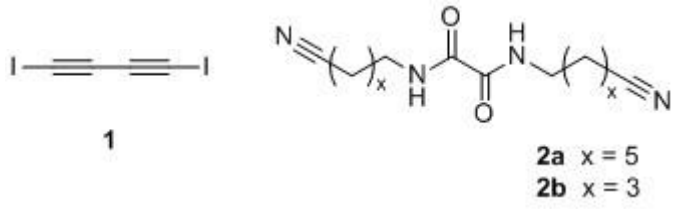

Figure 2.7 Diiodobutadiyne (left) and host compounds (right).

Sun et. al., analyzed the crystal structure of **1** and **2b** through x-ray diffraction methods and found that the polymer strands had a repeat distance of 4.94 Å, well within the range for 1-4 topchemical polymerization.[7] In addition the host nitriles were halogen bonded to the iodine atoms, however, the iodine atoms seem to be in close contact with the oxygen atoms on the oxalamide host as well (**Figure 2.8**) and though not too significant, contribute to its crystal packing structure. Multiple experiments were undertaken by our group to carbonize PIDA as the

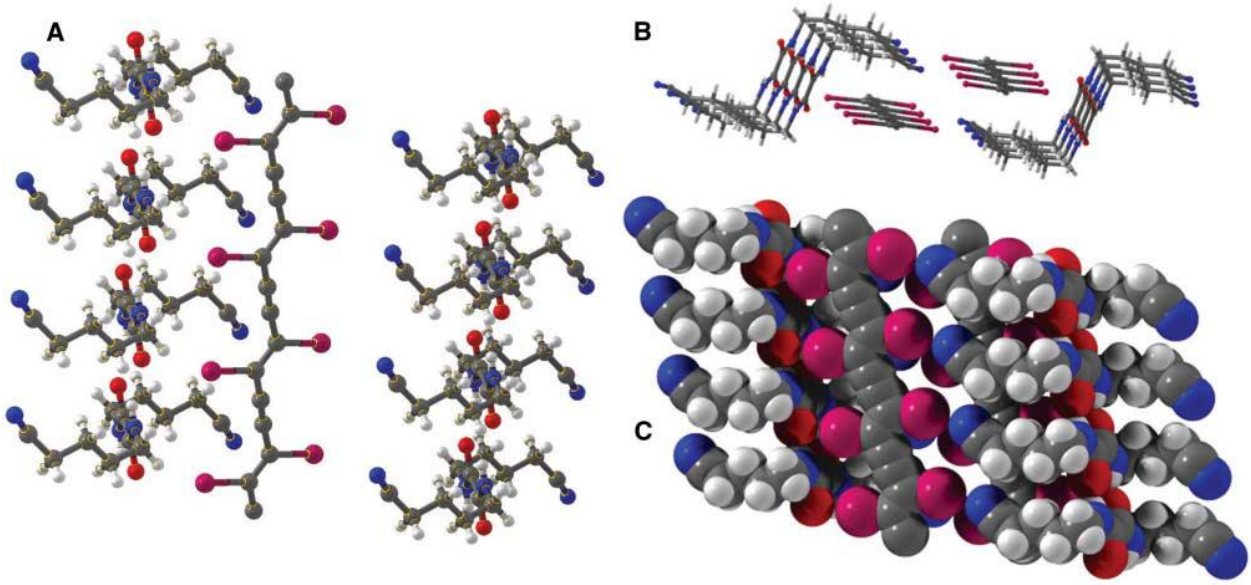

Figure 2.8 X-ray diffraction data of cocrystal **1** and **2b**. (**A**) A single chain of cocrystals, (**B**) top view in ball-and-stick model, (**C**) space filling representation. Reprinted with permission from [7]. Copyright [2006] Science.

first steps to produce carbyne, one of carbon's elusive allotropes that should be a high band-gap semiconductor.[39,40] Dehalogenation experiments and in turn, carbonization experiments especially were a main focus in order to explore PIDAs capability as a precursor for carbyne

2.3 Previous Work

Due to its simplicity in structure, PIDA could essentially be a precursor for an all carbon compounds. Previously, our group members focused on utilizing PIDA in order to create new graphitic materials and focused on the removal of its iodine substituents.[41] Dehalogenation of simple polymers should yield a simple, naked, carbyne chain with alternating sp and sp^3 bonds. In 1989, Evsyukov et al. studied dehydrohalogenation of poly (ethylene-alt-chlorotrifluoroethylene) (PE-a-CTFE) to make carbyne by treating the polymer with potassium tert-butoxide.[42] The theoretical synthesis is shown in **Figure 2.9**. However, full removal of the

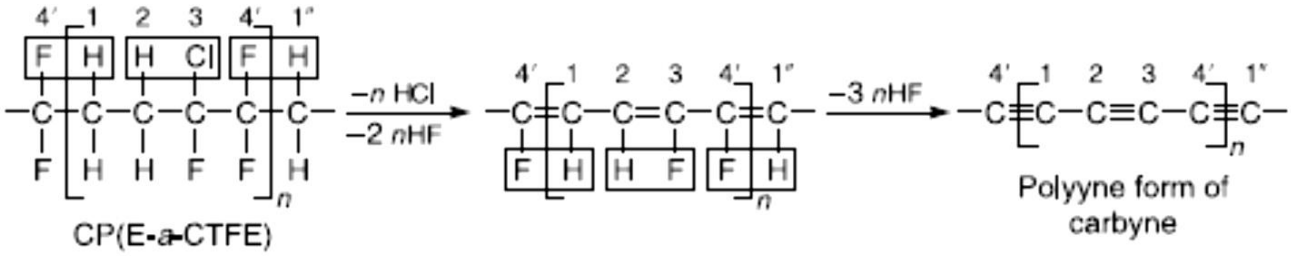

Figure 2.9 Dehydrohalogenation of PE-a-CTFE Copyright [14]

halogen was not achieved which could be the result of insufficient strength of the base, sterical hindrances and alternation defects in the original copolymer. A different reaction with the same basic concept, the dehalogenation of PIDA was attempted using several bases in order to carbonize the polymer into what would hopefully be a carbyne like material.

In order to separate PIDA from its host molecule, the polymer is suspended in an organic solvent, tetrahydrofuran or methanol, and results in a blue suspension (**Figure 2.10 B**).This blue suspension still has its UV-absorption peak at 680 nm indicating that PIDA is still intact. When the suspension is centrifuged, it separates into a colorless supernatant layer and a bulk mass of solid fibers is obtained which was identified as the isolated polymer.

Lou et. al found that PIDA can also undergo carbonization under thermal conditions at 900^{o}C as well as visible wavelength laser irradiation at room temperature.[13]At room temperature it was found that with the addition of a lewis base like pyrrolidine, pyridine or triethylamine de-halogenated the polymer, however, there was only a 60% loss of iodine from the material. The product could not produce any x-ray diffraction data, indicating that it was disordered. None of these methods allowed for a controlled elimination.

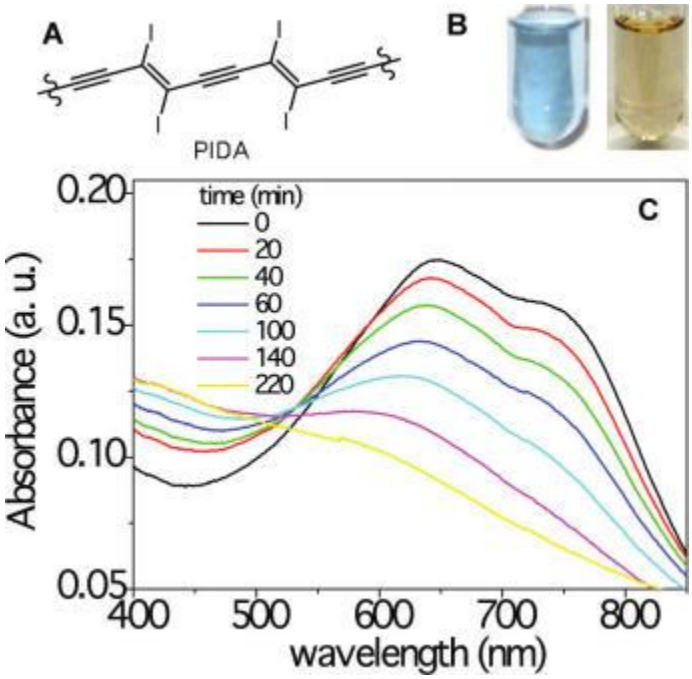

Figure 2.10 Polymer PIDA (A), the color change of the blue suspension of PIDA to the triethylamine added product (B), and the absorption spectroscopic change of the blue PIDA suspension after adding 0.1 mL triethyamine (C) Reprinted with permission from [13]. Copyright [2011] American Chemical Society

In order to understand the mechanism of iodine elimination, Resch used multiple reagents in order to induce dehalogenation on small molecules. Base induced deiodination was first investigated using excess pyrollidine on, 4,5-diiodo-4-octene (**3**). Its facile conversion was attributed to the halogen bonding between the Lewis-basic nitrogen of pyrrolidine and the Lewis-acidic iodine.[43] Solvent parameters were determined in this study and found that the deiodination is in fact solvent dependent and requires polar solvents. In addition, extensive kinetic analysis of

the elimination of iodine using pyrollidine showed that the elimination is not instantaneous and that a quartnary ammonium species forms (**Figure 2.11**).

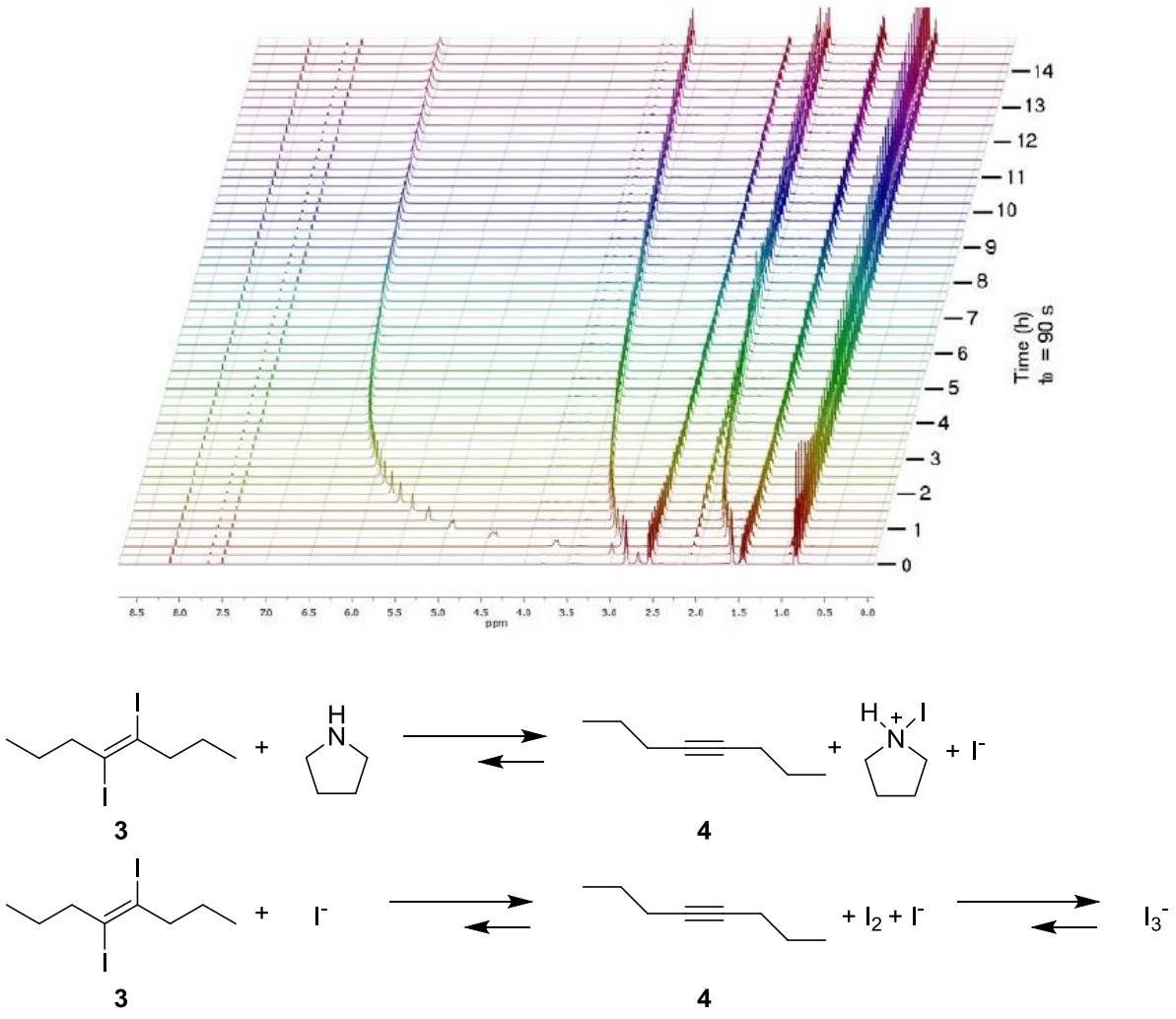

Figure 2.11 NMR kinetic profile (top) and proposed mechanism for the dehalogenation of compound **3** using pyrrolidine (bottom).[43]

In addition, halide nucleophiles, hydroxide and amines were all found to induce dehalogenation in E-iodoalkynes. The prosed mechanism for the deiodination for iodoalkynes is summarized below **Scheme 2.1**.[43]

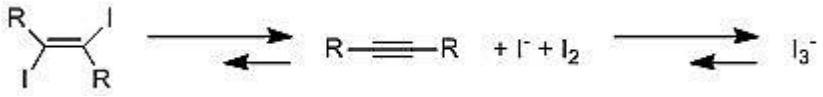

Scheme 2.1 Proposed mechanism for the deiodination of iodoalkynes.[43]

In previous experiments by Lou, iodine elimination from PIDA was carried out on isolated polymer. In order to isolate the polymer the cocrystals are placed in organic solvents (THF, methanol, etc.) and sonication for a given period of time. The issue that arises with isolated PIDA is that it starts to form aggregates to which only the surface strands are able to react with reagents added to the reaction flask. Daniel Resch, in order to combat the aggregates, used PIDA in its cocrystalline form instead.[43] By keeping the polymer in its ordered form, the reaction can proceed while the polymer strands are exfoliated from the surface of the crystals via the host solubilizing into the solvent. Iodine elimination experiments carried out by Daniel Resch is summarized in **Table 2.1**.

Reagent (eq.)	Solvent	Reaction Time (h)
Pyrrolidine (5000eq)	H_2O	24 h
Pyrrolidine (663 eq)	MeCN	48h
TBAI (500eq)	$MeNO_2$	24 h
TBAI (500eq)	EtOH-H2O 1:1	24 h
TBABR (500eq), $Na_2S_2O_3$ (500eq)	MeOH-H_2O 1:1	48 h
TBABR (500eq)	MeCN	48h
TBAI (500eq)	MeCN	24h
KI (500eq)	MeCN	24h
TBABr (500eq), $NaHSO_3$ (500 eq)	MeNO2:H2O 1:1	48 h
P(Ph)3 (250eq)	MeCN:H2O 10:1	24h
CH_4N_2S (250eq)	MeCN	48h

Table 2.1 Summary of the elimination experiments carried out by Daniel Resch [[43]] on PIDA cocrystals.

The majority of the results from Resch's work found that complete iodine elimination was not always achieved. In fact, though elimination occurred in every reaction conducted, iodine was still present in large quantities in every product except for the pyrrolidine reactions. When attempts to use reducing agents to eliminate iodine from PIDA were used, it was found in the EDS spectrum that heteroatoms were included in the material as well as the remainder of

iodine in the product. Resch attributed the large presence of iodine to the possibility that iodine could also act as a reducing agent.

If PIDA is able to absorb heteroatoms after the elimination of iodine, the process could be manipulated to incorporate a desired heteroatom like nitrogen. Using an azide as a source, PIDA could essentially undergo an elimination reaction and adsorb nitrogen molecules from an azide source. By trapping nitrogen in an amorphous carbon structure, it could be possible to manipulate the material through pressure induced experiments in order to achieve a carbon nitride-like material.[23, 26, 44]

Chapter 3- Dehalogenation of PIDA

3.1 Iodine Elimination with small molecules

PIDA is potentially a precursor to carbon nitride-like materials due to the weak C-I bonds that can easily be broken and its uptake of heteroatoms. It is possible to incorporate nitrogen into the polymer using a nitrogen source like azides for the elimination of iodine. Therefore, understanding the fundamental chemistry of iodine elimination by the use azides is important in order to optimize the conditions. Studying conditions using PIDA cocrystals, however, is very expensive and exceptionally time consuming. Instead, the small molecule previously used by Dan Resch, 4,5-diiodo-4-octene (**3**), was utilized in order to find the appropriate conditions(**Figure 3.1**). [43]

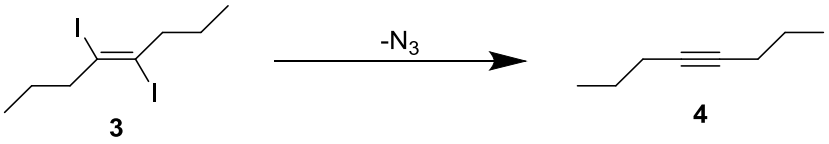

Figure 3.1 Model reaction using an azide to deiodinate 4,5-diiodo-4-octene

Previous experiments by Resh utilized a variety of reagents in order to induce iodine elimination in small molecules. Multiple iodo-alkenes were proposed however 4,5-diiodo-4-octene (**3**) was the most facile to work with because it can be distinguished from **4** by ^{13}C-NMR.The disappearance of the peak at 102.1 ppm signals the deiodination of **3** to alkyne **4**.

Azides in particular are known to react with iodine in a well-known reaction as illustrated in **Equation 1.**[45] However, the relationship between iodine and azides is utilized more in the determination of sulfur containing biological molecules, such as the monitoring of thioguanine in quality control experiments for cancer research.[46] Organic sulphides, thiocyanates, carbon disulphide, tri-, tetra-, and pentathionates act as catalysts when added to a solution containing

azide and I_2. Because PIDA seems to uptake heteroatoms or reagents, sulfur compounds were excluded from both small molecule experiments and all reactions with PIDA.

$$2\ N_3^- + I_2 \rightarrow 3\ N_2 + 2\ I^- \qquad \textbf{(Equation 1)}$$

The release of nitrogen gas is especially appealing because unlike the use of other reagents in the elimination of iodine, nitrogen gas leaving the solution or remaining is relatively harmless. When using sodium azide with I_2, the equation is as seen in **Equation 2**:

$$2\ NaN_3 + I_2 \rightarrow 3\ N_2 + 2\ NaI \qquad \textbf{(Equation 2)}$$

Polar, aprotic solvents like dimethyl sulfoxide (DMSO) or dimethyl formamide (DMF) are usually used to create a homogeneous mixture and increase the reaction rate. However, the high boiling points of DMSO and DMF make extraction and purification difficult. Therefore as an initial experiment the azide salt, tetrabutylammonium azide, was preferred due to its higher solubility in organic solvents.

As a model reaction to test the conditions and reaction time, 3 mL of deuterated solvent was used to create a dilute solution (0.2 M) of **3**. The reaction was monitored via TLC as well as NMR spectroscopy. Interestingly, the R_f value of **3** is 0.75 in hexanes while the R_f value of **4** is 0 in hexanes, making the reaction easy to monitor with TLC. The carbon NMRs were inspected for the alpha carbon peak **3** at δ 101.2. If the peak at δ 101.2 is present, the reaction had not gone to completion and the alpha hydrogens of **4**, δ 2.08 and **3**, δ 2.68, were then integrated and compared to obtain the percent conversions. No reaction that used tetrabutylammonium azide was able to proceed to complete conversion. In addition, when excess tetrabutylammonium azide was used, the reaction proved to be difficult to monitor via NMR without extracting the organic material due to the large butyl peaks. Sodium azide, however, possessed no carbons and thus could easily be used to monitor the reactions without the need of an isolated compound.

Sodium azide, though initially avoided due to its higher reactivity than tetrabutylammonium azide, was then tested with various organic solvents. The reaction was thus modified slightly to include a 1:1 ratio of azide to 15-crown-5 in order to increase its solubility in solvents, and azide ratios were adjusted. In acetonitrile there was a color change within 30 minutes, and all solvents were observed to have a significant color change by hour 3, as can be observed in **Figure 3.2**.

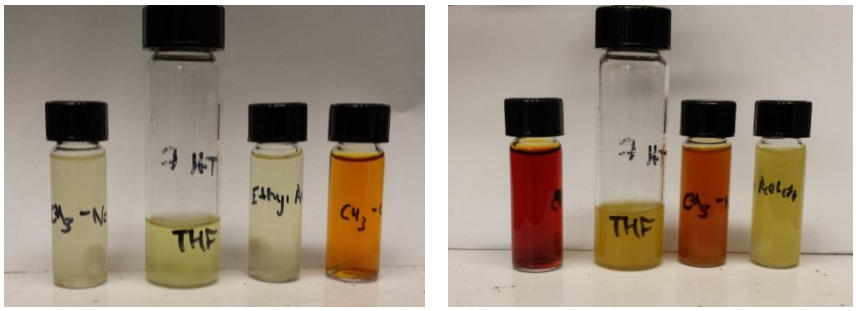

Figure 3.2 Comparison of color change of NaN_3 and **3** in various solvents at 30 minutes (right) and 3 hours (left). Note that the acetonitrile and ethyl acetate solutions were switched between the two photos.

The ideal conditions occurred in nitromethane with 2 eq. of NaN_3 to 1 eq. compound **3**. Tetrahydrofuran (THF), ethyl acetate as well as acetonitrile solutions reacted within a few hours, however only 1 eq. of azide was added into the vials and the reactions were not able to go to completion. **Table 3.1** summarizes the compiled results of the use of different solvents and azides.The reaction in nitromethane reached completion the quickest amongst the solvents that were used when it monitored with TLC. When extracted with ethyl acetates and washed with water, the NMR of the isolated product showed no starting material.

Solvent	Azide	Eq. of Azide	Elimination/Completion[c]
Acetone[d,e]	$N(But)_4N_3$	4	Yes/No
Acetonitrile[e]	$N(But)_4N_3$	4	Yes/No
DMSO[e]	$N(But)_4N_3$	4	Yes/No
Nitrobenzene[e]	$N(But)_4N_3$	4	Yes/No
Acetonitrile[a,b]	NaN_3	1	Yes/Yes
Ethyl Acetate[a,b]	NaN_3	1	Yes/No
Methanol[b]	NaN_3	4	Yes/No
Nitromethane[a,b]	NaN_3	1.5	Yes/Yes
Tetrahydrofuran[a,b]	NaN_3	1	Yes/No

Table 3.1 Iodine elimination from alkene **3**. a) 15-crown-5 was added to increase solubility of salt b) Sodium thiosulfate was added as a catalyst c) Monitored by TLC (silica/hexanes; R_f of **3** = 0.75 R_f of **4**= 0 d) Yielded neither the starting material nor product e) Deuteratehed solvents were used

3.2 Experiments on PIDA

PIDA can potentially be a precursor for new carbon and nitrogen rich materials because the C-I bonds are easily severed and the use of an azide can lead to the uptake of heteroatoms. Thus if the complete deiodination of PIDA can be achieved and the inclusion of nitrogen atoms can be accomplished, a new carbon-nitrogen material could be produced.

Originally the model experiments utilized a small ratio of sodium azide to 4,5-diido-4-octene **7**. However, it proved difficult to react the inner layers of the polymer PIDA with the azide when 1:4 equivalents of PIDA cocrystals and sodium azide were added to a solution of nitromethane and 15-crown-5. There was no change in color of the reaction medium as had been apparent in previous model exercises where the solvent turned orange. The azide content was raised to 200 eq. and the reaction was set to stir for a month (Procedure A).

With 200 equivalents of azide added, the solvent then turned a distinct dark orange after 2 days. After a month's reaction and centrifuging the solution down a black solid was obtained. When the black solid was washed with water and hexanes, an IR was taken and compared to the known IR spectrum of every other reagent used in the reaction; sodium azide, 15-crown-5 and

the host **2b** (**Figure 3.3**). The solid obtained had a broad peak around 3300 cm^{-1} corresponding to an O-H stretch, the black solid having absorbed water perhaps. A slight peak at 2900 cm^{-1} is indicative of a C-H peak and the rest of the peaks are overshadowed by a large background signal. The spectrum of the black solid does have small peaks that match the IR spectra of sodium azide and further compelled us to get a Raman Spectrum of the solid in order to determine any structural characteristics. (**Figure 3.4**).

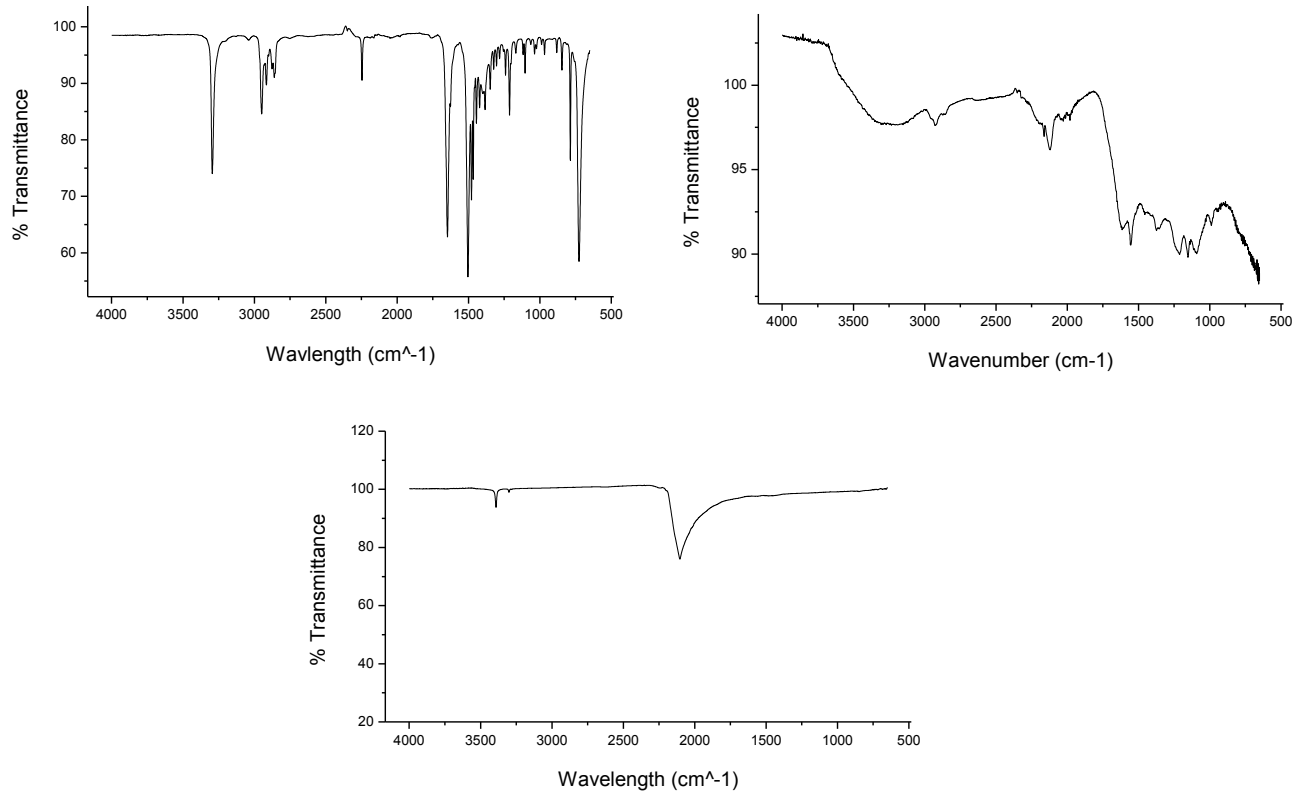

Figure 3.3 IR spectra of host **2a** used for cocrystalization (top left), the black solid obtained (top right) and sodium azide (bottom)

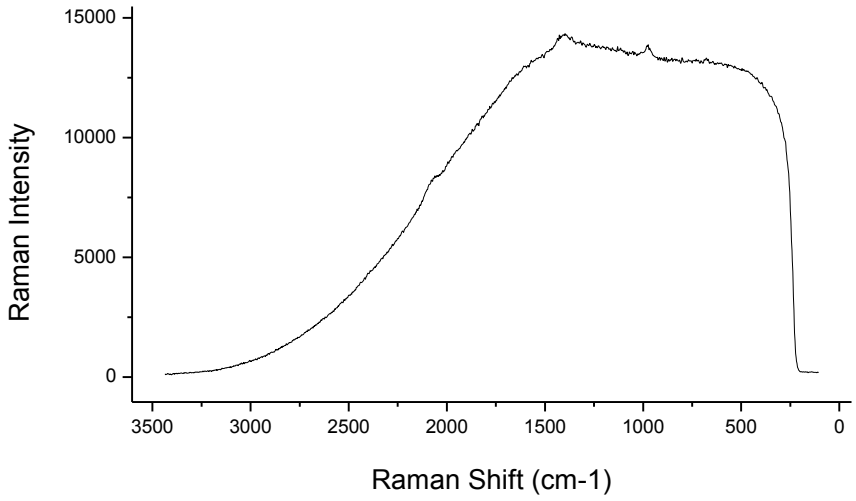

Figure 3.4. Raman of the black solid. Peaks at around 2000, 1600, and 1000 cm^{-1}

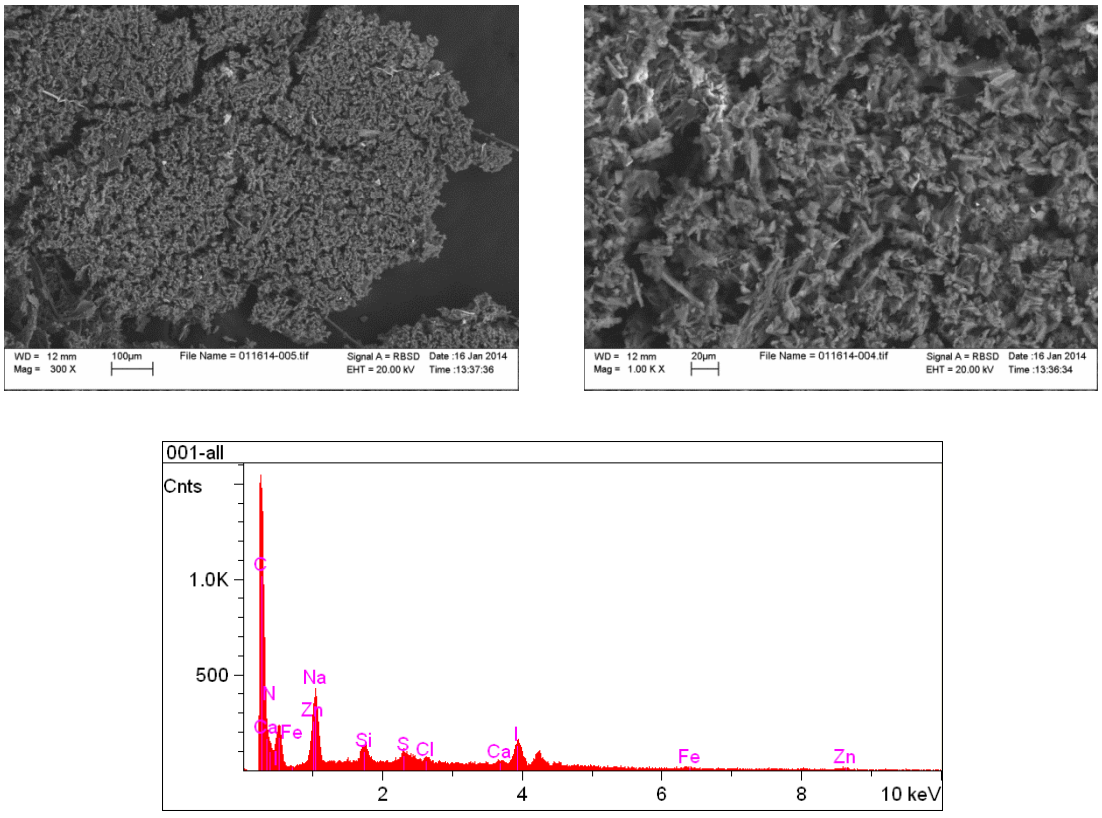

Figure 3.5 Top left: SEM of a large cross section of the solid. Top right: Magnified cross section. Bottom: EDS Analysis of large cross section

The Raman spectrum showed three small peaks at around 2000, 1600, and 1000 cm^{-1}. These small bumps, however, are barely visible due to the large photolumiscense background. The SEM shows the presence of small bright rod like structures associated with PIDA and the EDS analysis shows the much reduced presence of iodine (**Figure 3.5**). However there is the existence of nitrogen as well as sodium and other trace metals. In addition there were small fibrous materials present. It seemed that as the black solid dried, even when covered it accumulated outside particulates. In order to obtain a larger amount of material for further elemental analysis, the reaction was carried on a larger scale.

The second reaction (Procedure B) consisted of thoroughly washing a 100 mg sample of PIDA cocrystals after the reaction of sodium azide as well as sonicating between washes so that any remainder of unwanted particulate could be solubilized in the water or acetone. This sample, however, was only allowed to react for 5 days before processing in order to ascertain the impact of exfoliating strands. The process included using acetone and water and sonicating before centrifugation. The same type of polypropylene tubes was used, as well as the same type of crystallization dishes to dry the solid. However, the samples were drastically different from one another. Instead of forming chunks of aggregates, the second sample looked as if it formed a film and the edges proceeded to curl. The SEM (**Figure 3.6**) illustrates this characteristic.

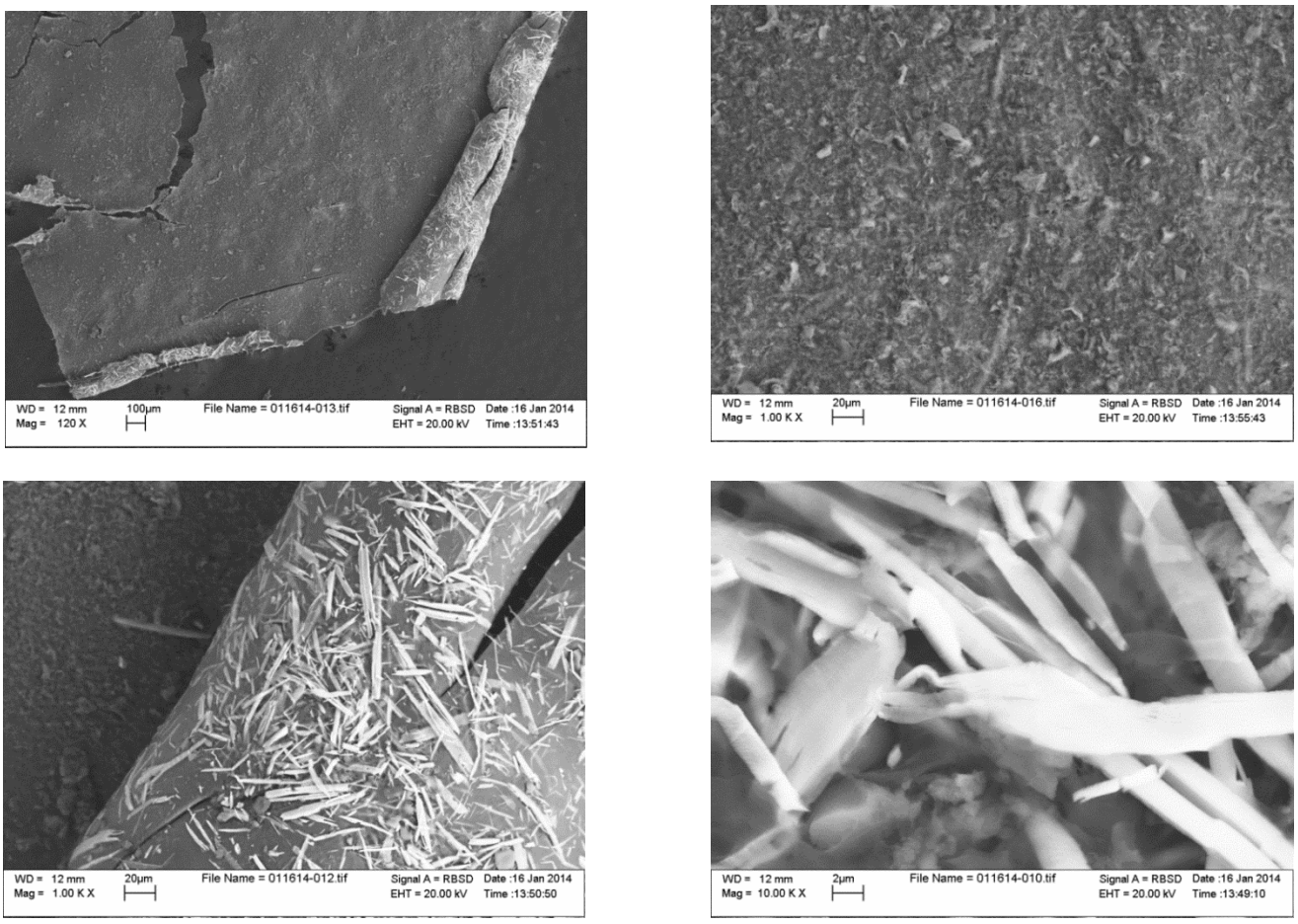

Figure 3.6 Top left: Illustrating the curl of what looks like a film. Top right: Zoomed into the top of the sample. Bottom left: zoomed into the underside of the sample that has curled up. Bottom right: Zoomed into the large crystalline fibers on the underside of the sample.

In conjugation with the EDS analysis (**Figure 3.7**), it appears that the underside of the sample is intact PIDA polymer due to the large amounts of iodine content in that area. However, what's interesting about this sample is that it was reported to have large amounts of fluorine. There were no fluorinated chemicals used nor any Teflon used in the experiment. Without further elemental analysis it cannot be fully assumed its elemental content, however, it is certain that there is still large amount of iodine present in the sample, presumably due to the shorter reaction time. The technique used in this reaction needs to be recreated in order to see whether or not the same results are reproduced. It should, however, be noted that the presence of sodium is

decreased and that sonication may have assisted in its removal. However, the presence of nitrogen does not seem apparent but cannot be ruled out without an elemental analysis.

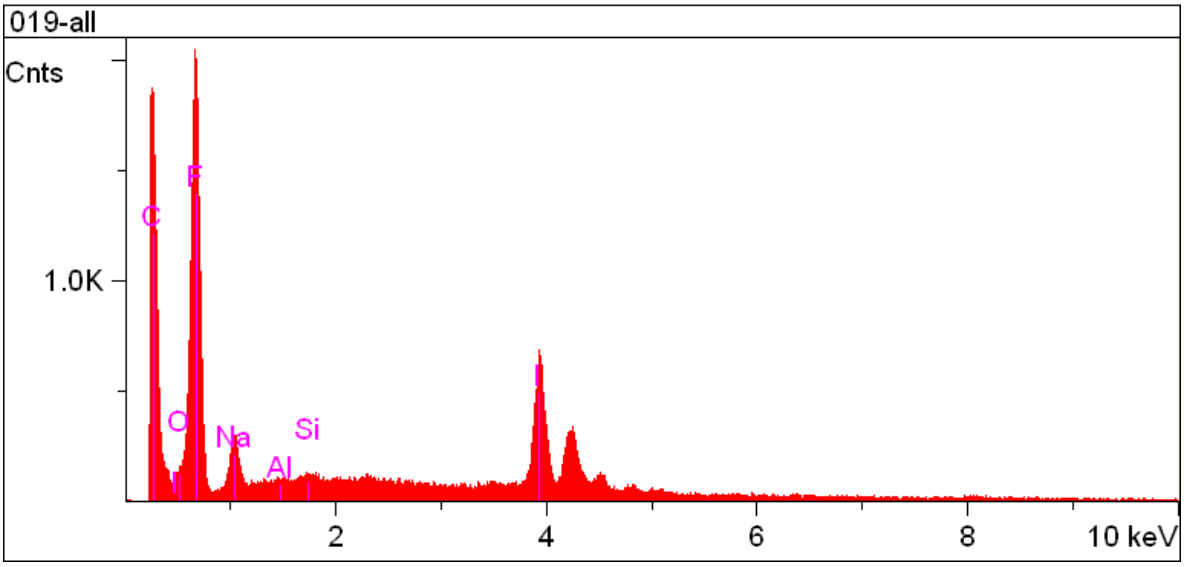

Figure 3.7 EDS analysis of second sample of PIDA cocrystals that were sonicated before washes of acetone and water.

With the large abundance of iodine present and the introduction of fluorine, it was determined that the previous procedure would need to be repeated. The next attempt (Procedure C) allowed the reaction to stir for a month. After 5 days' time the solution was divided up into 4 polypropylene tubes and centrifuged so that the remaining solid separated. The solvent was decanted and a fresh solvent of either acetone or water was added and sonicated in order to thoroughly wash the remaining solid. Optical images of Sample C are shown below in **Figure 3.8**.

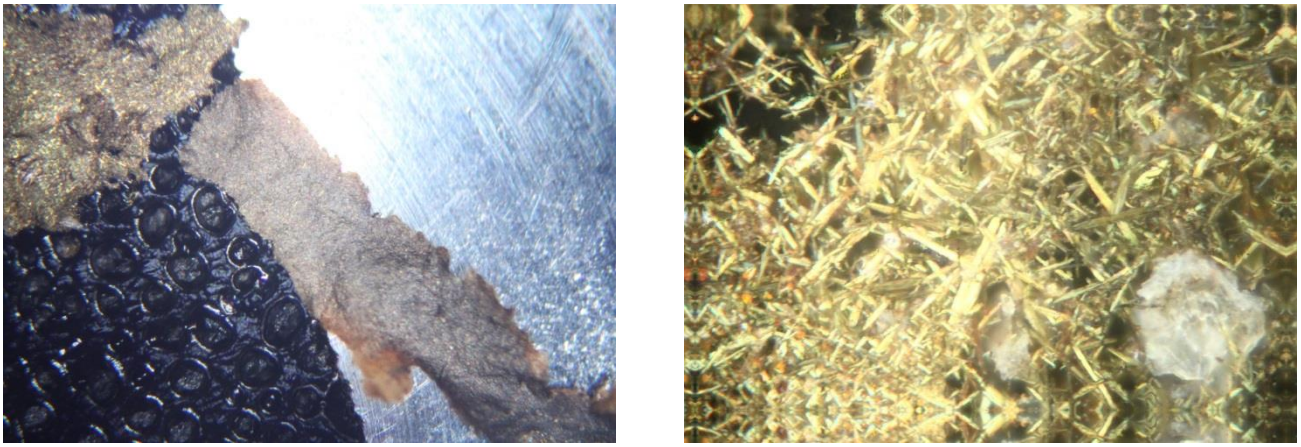

Figure 3.8 Optical images of what appeared to be a dark solid (left) and its magnification at 100x showing the existence of the golden PIDA cocrystals.

Sample C showed characteristics that the previous samples both possessed and more interesting features that they lacked. Like the Sample B that was only reacted for a short period of time and formed what appeared to be a film, Sample C looked as if it too had formed what appeared to be a film with curled edges (**Figure 3.9**). Though highly fluorescent due to the large amounts of iodine functionalities from the unreacted PIDA cocrystals which were present in the EDS (**Figure 3.10a**), there were darker areas on the SEM that were promising. In the EDS analysis taken of this area there was little to no iodine, trace amounts of metals and this dark area was composed mostly of carbon. (**Figure 3.10b**).

Due to the fact that the optical images, the SEM images as well as the EDS analyses show that the PIDA cocrystals are still intact and unreacted, it was expected that a Raman spectrum of the sample would also reveal the three main peaks associated with PIDA(around 2000, 1600, and 1000 cm^{-1}). **Figure 3.11** pictures the three familiar peaks as well as two small peaks at 2800, and 2300 cm^{-1}. The Raman peak at 2300 cm^{-1} could possibly relate to a C-N stretch previously found in carbon nitride networks. The Raman and IR classifications of carbon nitrides are not directly due to CN, NN, and NH vibrations.[47] However, due to the large amounts

of cocrystal still present in the solid, periodic sonication was thought to exfoliate the strands in order for the azide to react, even though bits of silica were reported to enter the solution from the rbf.[43]

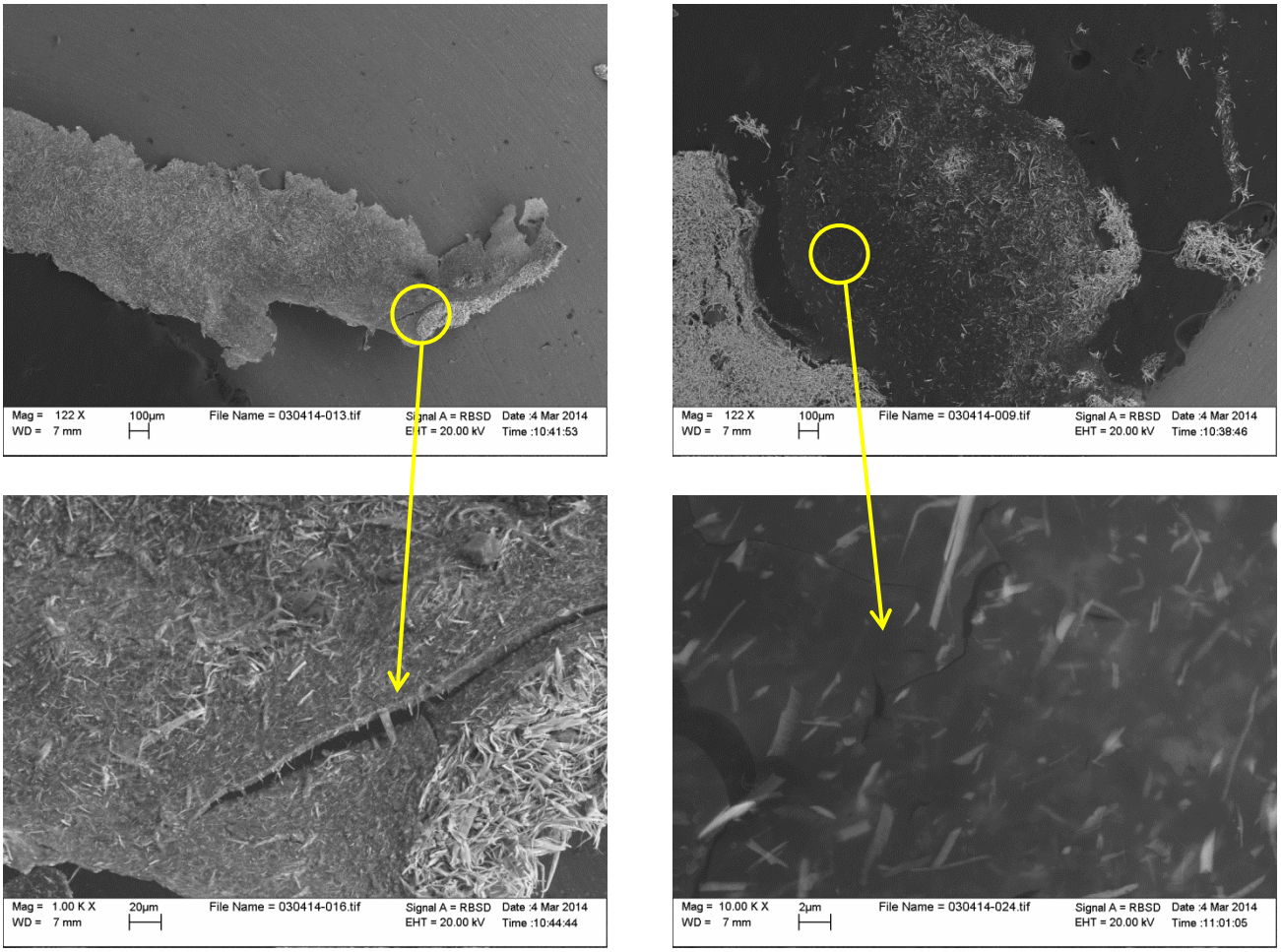

Figure 3.9 (Top left) SEM image of a cross section of Sample C. (Bottom left) Magnification of the cross section where there was a tear in the 'film'. (Top right) SEM image of a darker cross section on Sample C, (bottom right) the magnification of the darker cross section.

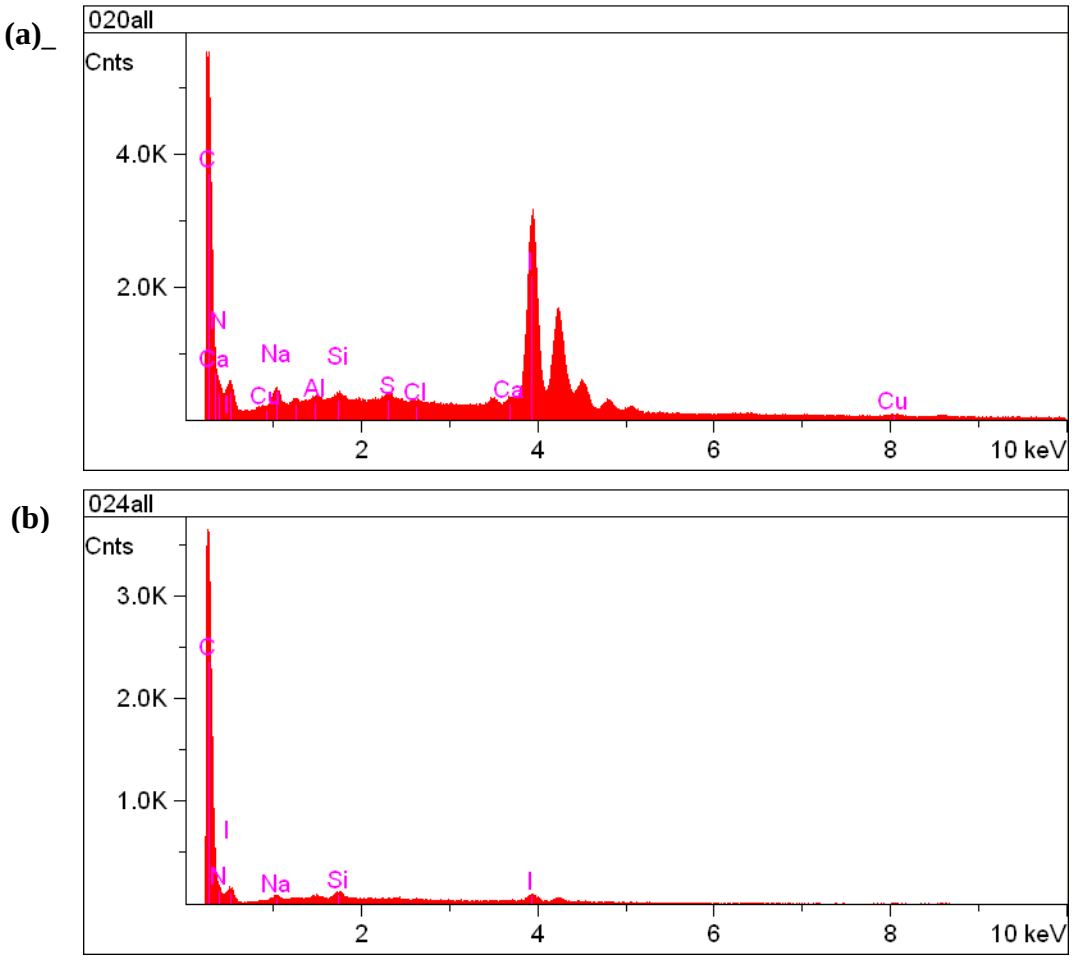

Figure 3.10 (a) EDS analysis of the bright section indicated on **Figure 3.9**, (b) EDS analysis of the darker section of Sample C.

The fourth experiment increased the equivalences of sodium azide (750 eq) and 15-crown-5 relative to PIDA cocrystals. The same washing technique was implemented and the rbf was sonicated periodically throughout the week (Procedure D). After a month long reaction, the solution was divided into four polypropylene tubes, centrifuged, and the remaining solid was washed with acetone and water. It was predicted that the amount of solid that would be obtained would be similar to that of the previous experiments (>1 mg). There was such a minimal amount of solid produced that the washing procedure was reduced from eight washed to six in fear of

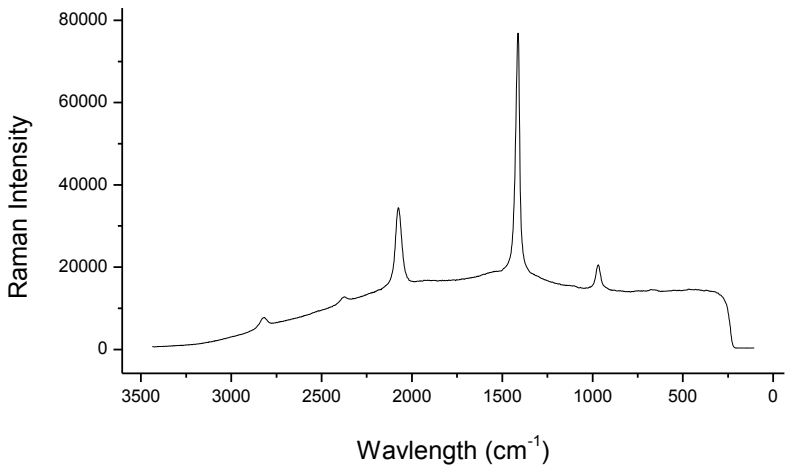

Figure 3.11 Raman spectrum of Sample C.

losing what little solid was obtained (Sample D). An SEM/EDS analysis was performed in order to determine the surface morphology of the solid (**Figure 3.12**).

Unlike the previous samples, Sample D did not have a large amount of iodine; however, there was a higher abundance of other trace metals, silicon and fluorine than any of the previous samples. Therefore the polymer must have broken either down or solubilized within the nitromethane solution. The orange solution of nitromethane was rotovaped down and what remained was a light orange solid/oil. The IR taken of the orange solid showed peaks at 3300, 2800, 2000, and 1100 cm^{-1}(**Figure 3.13**) All other peaks besides the peak at 2000 cm^{-1} are present in the IR spectra of the nitromethane solutions obtained in the other 3 experiments. However the peak at 2000 cm-1 is attributed to an azide stretch and its presence could be due to solubility issues of the large equivalence of azide. The orange solid/oil was then washed with water and extracted with ethyl acetate. The product obtained from the extraction was a very light orange crystalline material. An IR of this solid showed only the presence of the host **2a** used for cocrystallization (**Figure 3.14**). The Raman also gave no distinct peaks (**Figure 3.15**).

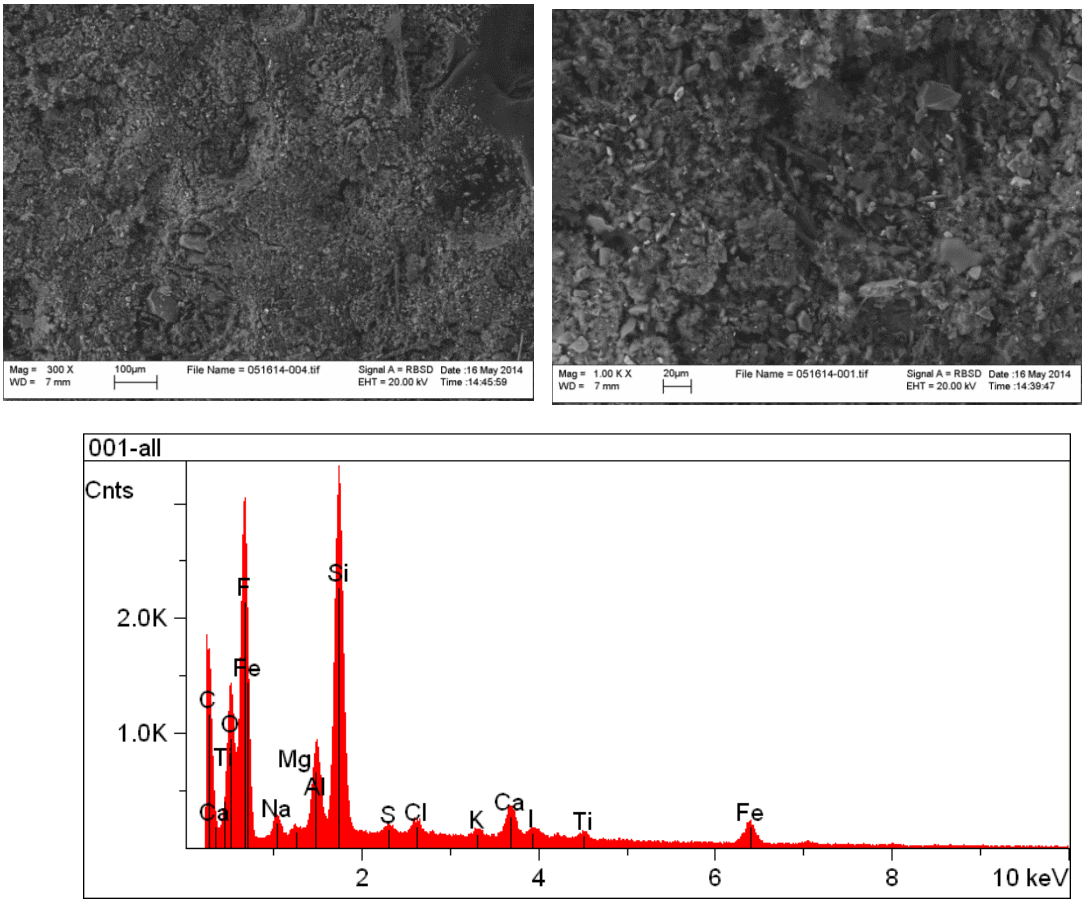

Figure 3.12 SEM images of Sample D (top) and the EDS analysis (bottom)

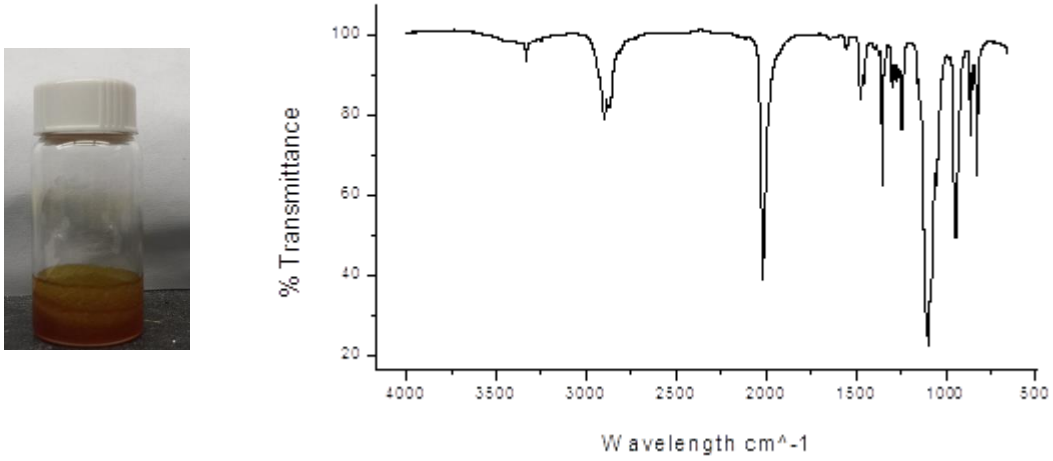

Figure 3.13 Orange solid obtained from the nitromethane solution of Sample D (left) and the IR spectrum of the orange solid.

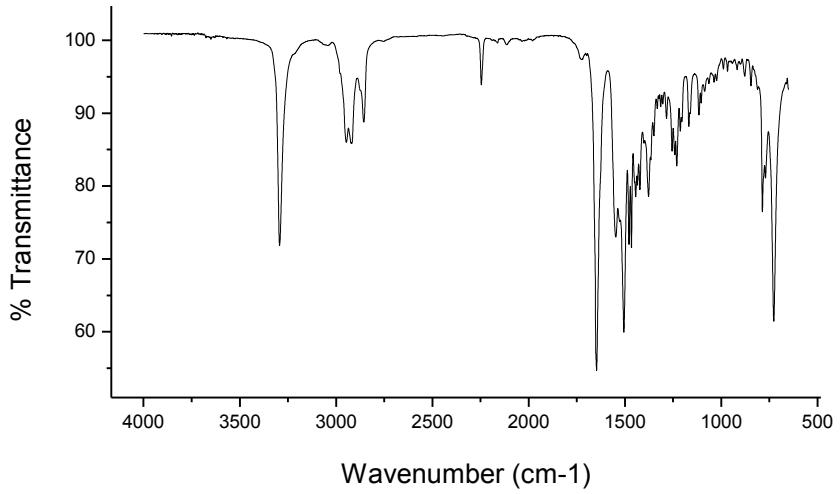

Figure 3.14 IR spectrum of the light orange crystals obtained from the nitromethane layer of Sample D.

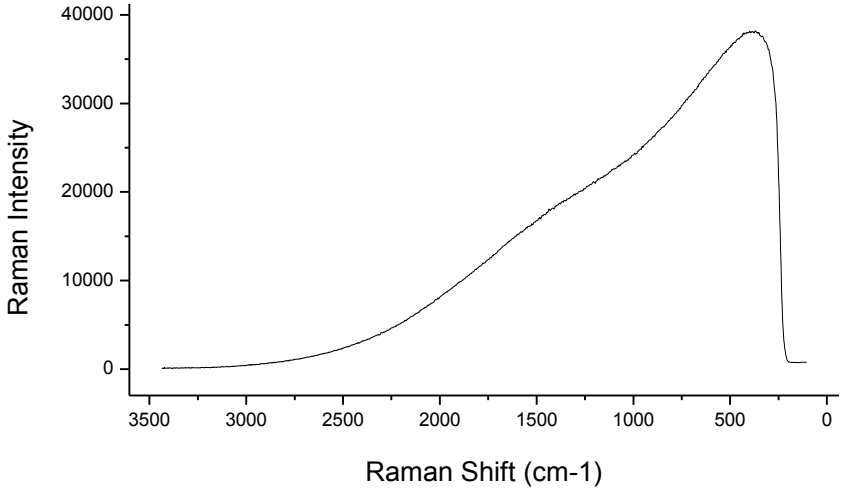

Figure 3.15 Raman spectrum of the light orange crystals obtained from the nitromethane layer of Sample D.

Multiple attempts to dehalogenate PIDA cocrystals by the use of sodium azide have failed to reproduce a fully deiodinated material. All attempts have also yielded different results and thus the deiodination could not be recreated (**Table 3.1**).

	Reaction Time	Eq. of NaN_3	Procedure	Appearance	EDS
A	1 month	200	Stirring	Black solid	Low in overall iodine
B	5 days	220	Stirring	Curled film	High in Iodine and Fluorine
C	5 days	220	Stirring	Curled film	High in iodine with areas of only carbon composition
D	1 month	750	Stirring with periodic sonication	Black solid	Trace metals, little to no iodine, little carbon species

Table 3.2 A comparison of all four reactions.

However, of the methods, simply stirring cocrystals without sonication appears to give the best results (Sample C); it has the least amount of impurities in the EDS analysis and though it does have a large amount of iodine present, it was the only sample to give a signal besides PIDA in the Raman spectra. Obtaining an elemental analysis for Sample C as well as performing electron mobility studies on the apparent film could prove to be an interesting area of study for further research.

3.3 Experimental

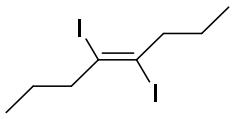

4,5-diiodooct-4-ene (3) : 4-Octyne (1.0121 g, 9.18 mmol) **3** was added to 15 mL Nitromethane followed by iodine (2.8101 g, 11.02 mmol) was added to the solution. The reaction was monitored via TLC until completion. 15 mL of deionized water was added to the reaction followed by extraction with hexanes (40 mLx4). The extracts were combined and was washed with 15% sodium thiosulfate (40 mL x2). The organic layer was dried with $MgSO_4$ and filtered

before rotary evaporation. The resulting yellow liquid (0.96 g) was collected in a yield of 95% . ^{1}H NMR (400 MHz, C6D12) δ 2.68 (t, 2H), 1.59 (dd, 7.4 Hz, 2H), 0.95 (t, *J* = 7.4 Hz, 6H); ^{13}C NMR (101 MHz, C6D12) δ 101.9, 53.3, 22.2,12.9.[1]

Elimination of Iodine with Tetrabutyl Ammonium Azide: In a vial, 3 mL of deuterated solvent (nitrobenzene, acetone, methanol, acetonitrile, or dimethysulfoxide) was added, followed by tetrabutylammonium azide (0.68 mL, 4.2 mmol). The mixture was allowed to stir for one minute. 4,5-Diiodooct-4-ene (0.09 mL , 0.6 mmol) was then added to the solution and allowed to react overnight. There was a color change observed, from light yellow to dark reddish brown. The contents of the vial were then transferred to an NMR tube and the triplets at 2.53 ppm corresponding to **3** and 2.06 ppm corresponding to **4,** were integrated to calculate the conversion percentage.

Elimination of Iodine with Sodium Azide: In a vial, 3 mL of solvent (nitromethane, ethyl acetate, tetrahydrofuran, and acetonitrile) was added, followed by sodium azide (85.8 mg, 1.32 mmol) and 15-crown-5 (0.26 mL,1.32 mmol). The mixture was allowed to stir for one minute until homogeneous. 4,5-diiodooct-4-ene (0.13 mL , 0.89 mmol) was added to the mixture and allowed to stir for 5 hrs. 10 mL deionized water was added, followed by extraction with hexanes (20 mL x2). The organic layer was dried over $MgSO_4$ and filtered before concentration *in vacuo*. The resulting product is a clear oil (0.31 g, 0.84 mmol). ^{1}H NMR (300Mz, $CDCl_3$) δ 2.06 (t, J = 7.2 Hz, 4H), 1.45 (m, J = 7.2 Hz, 4H), 0.96 (t, J = 7.6 Hz, 6H). ^{13}C NMR (300Mz, $CDCl_3$) δ 80.1, δ 22.7, δ 20.8, δ 14.1.

General Procedure for PIDA Cocrystals: Host **2a** (39 mg, 0.13 mmol) and diiodobutadiyne **1** (80 mg, 0.26 mmol) were dissolved in 12 mL of acetonitrile. The solution was sonicated to dissolve any remaining host or guest. The solution was divided into four crystallization dishes

and wrapped in foil with holes punctured to allow for slow solvent evaporation. Cocrystals were left to grow at room temperature for 2 days. General yields for cocrystals ranged from 60-90%.

Procedure A- NaN_3 I_2 Elimination in Nitromethane: In a argon-flushed rbf with 40 mL of CH_3NO_2 , polymerized cocrystals (56 mg, 0.062 mmol) of host were added. In a separate flask, 40 mL of CH_3NO_2 and NaN_3 (0.76 g, 11.75 mmol) and 15-crown-5 (2.76 g, 12.53 mmol) were stirred until solid dissolved in solvent. The azide solution was then added via syringe so the reaction. . The reaction mixture was allowed to stir for a month before being divided up into four polypropylene centrifuge tubes. The solution was centrifuged for 30 minutes at 2000 rpm. After the centrifuge the solvent was decanted and saved for later analysis. 20 mL of water was added into the tubes and centrifuged for 30 min. The liquid was decanted and the process was repeated four times. Hexane (20 mL) was added to each tube and centrifuged for 30 minutes. The liquid was decanted and the process was repeated four times. The liquid was decanted and the remaining black solid was washed out with acetone and left to dry in a crystallization dish. .Less than 2 mg of material was obtained.

Procedure B- NaN_3 I_2 Elimination in Nitromethane: In a argon-flushed rbf with 40 mL of CH_3NO_2 , polymerized cocrystals (90 mg, 0.099 mmol) were added. In a separate flask, 40 mL of CH_3NO_2 and NaN_3 (1.4 g, 22m mol) and 15-crown-5 (5 g, 0.022 mmol) were stirred until solid dissolved in solvent. The azide solution was then added via syringe. The reaction was allowed to stir for five days before being divided up into four polypropylene centrifuge tubes. The solution was centrifuged for 30 minutes at 2000 rpm. After the centrifuge the solvent was decanted and saved for later analysis. 20 mL of water was added into the tubes and then subjected to sonication for five minutes before centrifugation. The liquid was decanted and the process was repeated two more times. Acetone (20 mL) was added to each tube, sonicated for five minutes

and then centrifuged for 30 minutes. The acetone was decanted and the process was repeated four times. After decanting the liquid, the remaining solid was washed out with acetone and left to dry in crystallization dishes.

Procedure C- NaN_3 I_2 Elimination in Nitromethane: 50 mL of nitromethane was added to an argon flushed flask with PIDA cocrystals (99 mg, 0.11 mmol). In a separate flask, 30 mL of CH_3NO_2 and NaN_3 (1.4 g, 22 mmol) and 15-crown-5 (5 g, 0.022 mmol) were stirred until solid dissolved in solvent. The azide solution was then added via syringe and the reaction was allowed to stir for five days. After five days, the reaction mixture was divided up into four polypropylene centrifuge tubes. The solution was centrifuged for 30 minutes at 2000 rpm. After the centrifugation, the solvent was decanted. Water was added (20 mL) into the tubes and then subjected to sonication for 5 minutes before centrifugation. The liquid was decanted and the process was repeated two more times. Acetone (20 mL) was added to each tube, and then the tubes were sonicated for five minutes and then centrifuged for 30 minutes. The acetone was decanted and the process was repeated 4 times. After the liquid was decanted, the remaining solid was washed out with acetone and left to dry in crystallization dishes. The solid obtained was less than 2 mg.

Procedure D- NaN_3 I_2 Elimination in Nitromethane: In a argon-flushed rbf , 90 mL of CH_3NO_2 , PIDA cocrystals (134 mg, 0.15 mmol) were added. In a separate flask, 90 mL of CH_3NO_2 and NaN_3 (4.9 g, 75 m mol) and 15-crown-5 (18 g, 75 mmol) were stirred until the solid dissolved in solvent. The azide solution was then added via and the reaction was allowed to stir. The reaction mixture was sonicated every other day for the next month for 30 minutes each time. After a month, the reaction mixture was divided up into 4 polypropylene centrifuge tubes. The solution was centrifuged for 30 minutes at 2000 rpm. After the samples were centrifuged the

solvent was decanted and saved for later analysis. Water was added (25 mL) into the tubes and then subjected to sonication for 5 minutes before centrifugation. The liquid was decanted and the process was repeated two more times. Acetone (25 mL) was added to each tube; the tubes were then sonicated for five minutes and then centrifuged for 30 minutes. The acetone was decanted and the process was repeated four times. After decanting the liquid, the remaining solid was washed out with acetone and left to dry in crystallization dishes.

Washing of Nitromethane Layer of Sample D: 20 mL of the 216 ml nitromethane solution from Sample D was subject to rotary evaporation and concentrated *in vacuo*. The result was 2 g of an orange solid/oil. This crude solid/oil was analyzed by Raman and IR spectroscopy. The solid/oil was then dissolved in 50 ml of water and extracted with ethyl acetate (2 x 20 mL) and washed with water (4 x 40 mL). The product was then subject to rotary evaporation and concentrated *in vacuo* to yield light orang crystals (7 mg). The crystals were analyzed by IR spectroscopy which showed identical peaks for host molecule **2a** (3285 cm^{-1}, 2957 cm^{-1}, 2918 cm^{-1}, 2844 cm^{-1}, 2242 cm^{-1}, 1648 cm^{-1}, 1507 cm^{-1}). The Raman gave no clear results.

Chapter 4 - Organic Synthesis Study

4.1 Preparing PIDA

Though the synthesis of diiodobutadiyne is not difficult, there are specific precautions that must be undertaken in order to ensure proper cocrystallization with host and in turn polymerization. Synthesis of diiodobutadiyne and its polymerization are highly sensitive to environmental factors. The synthesis of the monomer **1** is carried out in the dark and **1** is stored in the dark due to its light sensitivity (**Scheme 4.1**)

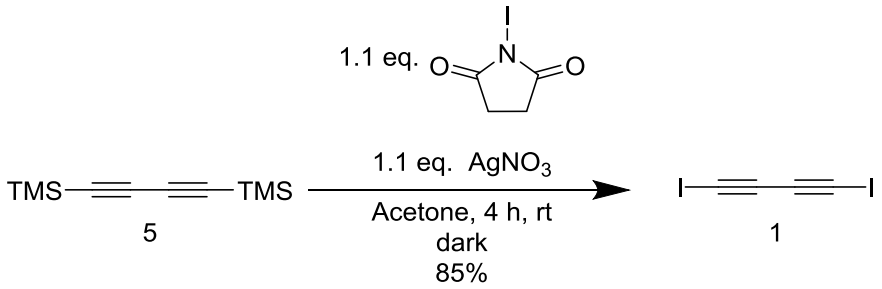

Scheme 4.1 Synthesis of Diiodobutadiyne **1**

In addition to its light sensitivity, diiodobutadiyne **1** is shock sensitive and thus should only be prepared in quantities less than 1 g to follow proper safety protocols. It should also always be stored in solution in the freezer and only be kept in the freezer for no more than 2 weeks to percent degradation of the polymer. If these precautions are adhered to, proper cocrystals formation with any host molecule will prove facile.

4.2 Scaling up Host Synthesis

The most common host used to cocrystallize with **1** is the oxalamide host **2a.** Previous work done by Daniel Resch of the Goroff group found that host **2a** showed the best yield in cocrystal formation with **1**.[43] It was determined that the long alkyl chain of **2a** imparted more

flexibility for the monomers and host molecule to form hydrogen bonds and meet the geometric requirements for 1,4-topochemical polymerization. Previously, Liang prepared **2a** according to **Scheme 4.2** pictured, below.[48]

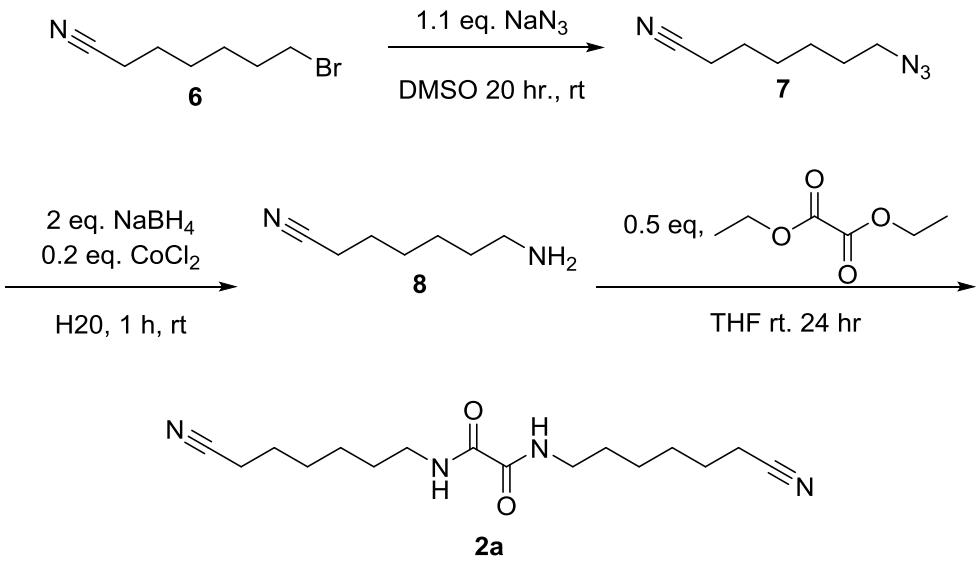

Scheme 4.2 Synthesis of 2a.[48]

Here the reducing agent used was $NaBH_4$.[49] However, when the reaction was scaled up to 5g from **7** to **8**, there was a large amount of heat generated; for safety reasons this was not repeated. However, due to a large demand of the host molecule for cocrystallization with other monomers in our group, Resch used the Staudinger reduction (**Scheme 4.3**) to avoid heat generation and continue the bulk synthesis of **2a** without heat generation.[43]

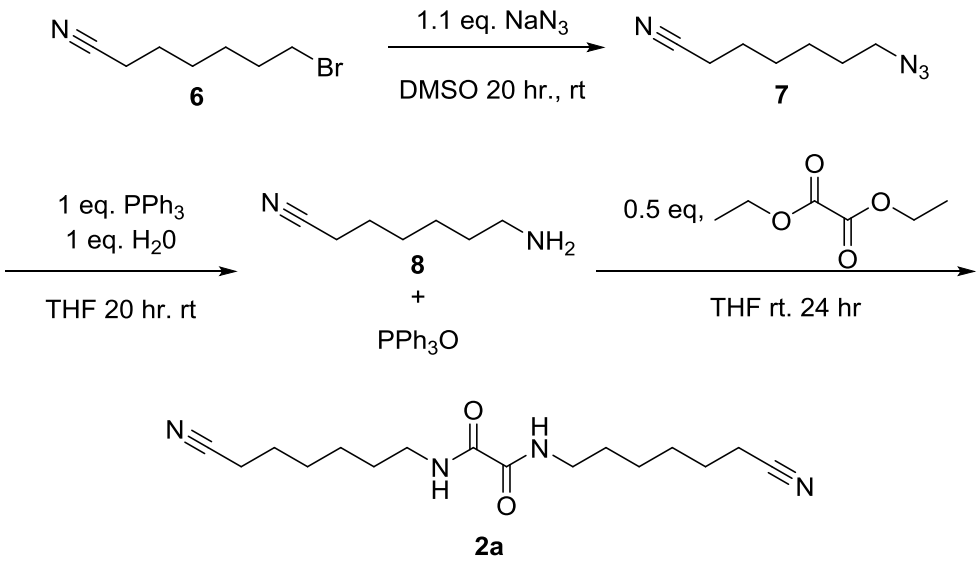

Scheme 4.3 Synthesis of 2a with Staudinger reduction

Recently, the Staudinger reduction proved to create impurities in the product of **8.** The triphenyphosphine oxide (PPh_3O) is an inert solid and relatively simple to remove from the reaction to obtain pure 7-aminoheptanenitrile **8**. HCl was used to protonate the amine and move it into the aqueous layer, the triphenylphosphine oxide remains in the organic layer. However, PPh_3O is slightly soluble in acid solutions as well. Though initially the presence of PPh_3O was assumed to be inconsequential do to its lack of reactivity, it may interfere with both the equivalence of host to guest needed for crystallization as well skew the crystal growth itself.

In order to overcome the presence of PPh_3O in the final products, a distillation of 7-aminoheptanenitrile **8** from the solid PPh_3O product was applied on a 10 g scale. At 2 torr PPh_3O has a boiling point between 226 – 230 ^oC.[50] This is much higher than compound **8** which has a boiling point of 108 – 110 ^oC at 2 torr.[51] The large difference between boiling points allowed the product to be distilled out without any impurities and at a 94% yield. The remainder of the procedure was carried out accorded to Resch's procedure to form **2a** (**Scheme 4.3**).

4.3 Push Pull Diynes

Conjugated polymers can yield interesting electronic and optical properties, as mentioned in **Chapter 2**. Used largely in photovoltaics in order to replace the silicon-based solar cells, conjugated polymers can be made in bulk.[52] In bulk heterojunction based solar cells, the common material for acceptors are the fullerene derivatives, specifically (6,6)-pheny-C_{61}-butyric acid methyl ester or (6,6)-phenl-C_{71}-butyric acid methyl ester.[52,8,6,4] The issue arises with the use of the donor material and its inability to deliver high power conversion efficiencies (PCE's). The failure of these donor polymers to deliver practical efficiencies is attributed to their narrow absorption spectra and their large optical band gaps.[52]

Push-pull conjugated polymers, or donor-acceptor polymers, have been targeted in order to combat the low PCE's of traditional homopolymers. Price et. al., synthesized a fluorine substituted conjugated polymers, which produced a PCE of 7%, applied with fullerene derivatives in a bulk heterojunction based solar cell. [53] Benzodithiophene was incorporated as the donor and the fluorinated benzotriazole was chosen as the acceptor module (**Figure 4.1**).

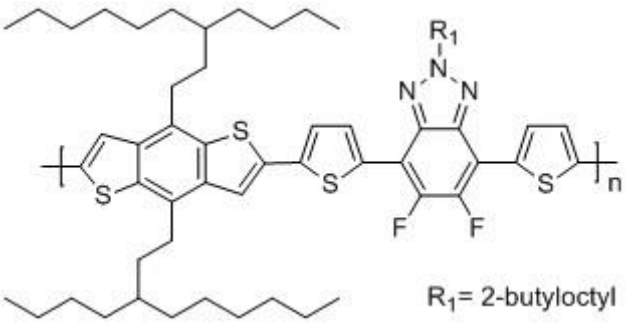

Figure 4.1 PBnDT-FTAZ

By utilizing the same concept of push-pull conjugated polymers, our group seeks to synthesize polyynes with electron donor and acceptor units and topochemically polymerize them in an ordered manner. Previously Rui Xu et. al., synthesized electron poor perfluorophenyl and electron rich phenyl end caped triyne monomers that interact to line up triyne monomers with

repeat distance and angles for topochemical polymerization.[54] Utilizing the host-guest techniques used to polymerize PIDA, it was believed that monomers end capped with the electron donating iodine and an electron withdrawing carboxylic acid group could interact with **2a** or **2b**. Interacting with **2a** or **2b** could line up new push-pull diynes with appropriate repeat distances and angles for topochemical polymerization.

Initially the monomer 4-(iodobuta-1,3-diyne-1-yl)benzoic acid was synthesized with a moderate yield by group member Xiuzhu Ang. The synthesis is summarized in **Scheme 4.4** below.

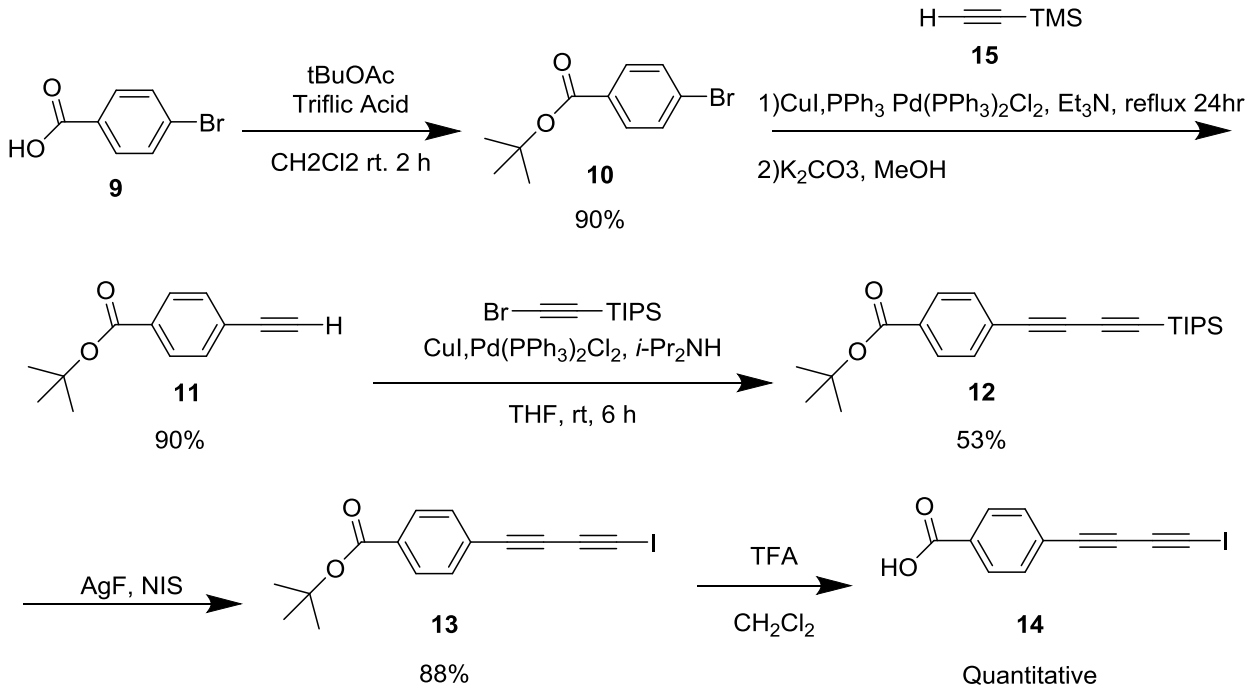

Scheme 4.4 Synthesis of 4-(iodobuta-1,3-diyne-1-yl)benzoic acid[15]

The initial step of attaching a t-butyl group to acid proved to be the first difficulty. Though reported at a 90% yield, when performed yields were closer to 20-40% for compound **10**.[55] Continuing onto the next step where a Sonogashira coupling was utilized to attach an alkyne, there was the same issue of low yield. To achieve only a 42% yield for compound **11** for what

should have been a more successful reaction created a dilemma; the reaction that would follow had a much lower yield and would diminish yields. For the Sonogashira, there was a large amount of homocoupling achieved of the acetylene **15**. In order to avoid homocoupling and achieve better reactivity of the t-butyl benzoic acid derivative, iodine was chosen as a substituent as opposed to bromine.[56]

Therefore 4-iodobenzoic acid was chosen as the precursor and it underwent an esterification. However, the original scheme of adding a t-butyl group proved to give low yields as well. A new route proven to give high yields (>90%) for iodobenzoic acids was adapted. Using oxalyl chloride to chlorinate and the desired t-butyl alcohol, 4-iodobenzoic acid could be esterfied.[57] The presumed synthesis is shown in **Scheme 4.5** below.

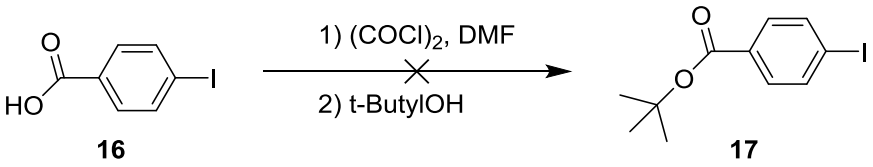

Scheme 4.5 Chlorination then esterification of 4-iodobenzoic acid

Initially the reaction did not proceed at all and it was attributed to the solvent (dichloromethane) not being dry and in turn cleaving the acetylchloride formed. However when the reaction was attempted in completely dry conditions as well as neat, the only product obtained was the starting material. In addition, the method for synthesizing compound **10** was also utilized in the synthesis for **16** (**Scheme 4.6**). Though the reaction did proceed, the yield was still low relative to Ang's procedure utilizing 4-bromobenzoic acid.[55]

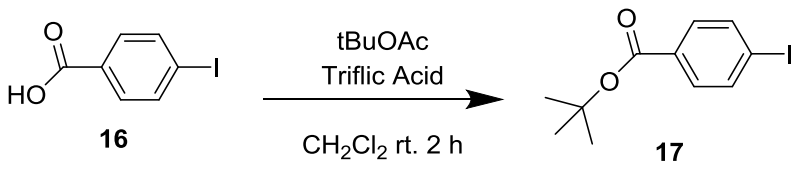

Scheme 4.6 Esterfication of 4-iodobenzoic acid

However, iodobenzoic acid was utilized in the Sonogashira coupling reaction in order to observe if the reactivity would increase (**Scheme 4.7**). Not only did the addition of the iodine substituent not increase yield, surprisingly no product beside the starting material was obtained. Due to the lack of material synthesized from failed yields, the synthesis towards 4-(iodobuta-1,3-diyne-1-yl)benzoic acid was halted.

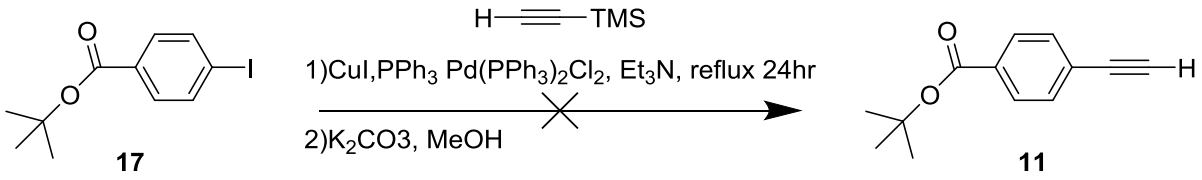

Scheme 4.7 Sonogashira coupling with 4-Iodobenzoic acid tert-butyl ester

Although the yields were lower than anticipated for the reactions that did succeed, there was a limited amount of time to fully synthesize the diyne which previous group members had succeeded in attempting. The push pull diyne, 4-(iodobuta-1,3-diyne-1-yl)benzoic acid, was synthesized and cocrystallized with **2b** by Xiuzhu Ang.[55] There are a number of different polyynes that can be synthesized and cocrystallized using a host guest strategy that could contribute to the study of push-pull polymers.

4.4 Experimental

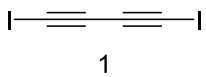

1

Diiodobutadiyne (1): 1,4-Bis(trimethylsilyl)butadiyne (0.500 g, 2.57 mmol) was added to an aluminum foil wrapped rbf. Acetone (125 mL) was then added to the flask. N-Iodosuccinimide (1.156 g, 5.14 mmol) and $AgNO_3$ (0.873 g, 5.14 mmol) were added to the solution. The reaction mixture was allowed to stir for 4 h before the solvent was removed *in vacuo* and 100 mL hexanes was added. The contents of the reaction flask were swirled and subjected to vacuum filtration. Water (100 mL) was then added to the filtrate and the liquid was transferred to a

separatory funnel. The hexanes layer was separated and fresh hexanes (80 mL) were added to the separatory funnel. The water layer was extracted using hexanes (3 x 40 mL). The organic layers were combined, dried with MgSO4, and filtered. The solvent was removed *in vacuo* to afford compound 1as a faintly yellow solid (0.7 g, 2.3 mmol) in 90% yield: ^{13}C-NMR (125 MHz, $CDCl_3$) δ 79.7, -3.4.[43]

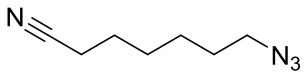

7

7-Azidoheptanenitrile (7): 7-Bromoheptanenitrile (11.89 g, 62.58 mmol) was weighed out into a flask and 160 mL dimethyl sulfoxide was added. Sodium azide (4.91 g, 75.53 mmol) was then added and the reaction mixture was allowed to stir for 24 hours. The reaction was then quenched with 100mL de-ionized water, followed by extraction with ether (4 × 100 mL). The combined ether layers were concentrated *in vacuo* to half volume, washed with water (4 × 100 mL), and finally the ether was removed *in vacuo*. The resulting faint yellow oil (3.80 g, 25.0 mmol) was obtained as compound **7** in 65% yield: ^{1}H NMR (300 MHz, $CDCl_3$) δ 3.28 (t, 2H), 2.35 (t, 2H), 1.77 – 1.53

(m, 4H), 1.53 – 1.07 (m, 4H).[43]

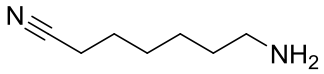

8

7-Aminoheptanenitrile (8): 7-Azidoheptanenitrile (6.16 g, 40.49 mmol) was dissolved in 60 mL of wet THF with triphenylphosphine (18.05 g, 68.86 mmol). Deionized water (3 mL) was then added to the flask, and the reaction mixture was stirred at room temperature for 48 hours.

After the 48 hours the solvent was removed *in vacuo*. The resulting product was a white solid. A clear oil was then distilled out of the reaction mixture at 160°C (4.83 g, 38.30 mmol) 94% yield: ^{1}H NMR (400 MHz, $CDCl_3$) δ 2.68 (t, *J* = 6.8 Hz, 2H), 2.33 (t, *J* = 6.9 Hz, 2H), 1.64 (dd, *J* = 15.2, 7.2 Hz, 1H), 1.57 – 1.30 (m, 3H), 1.27 (s, 1H).[43]

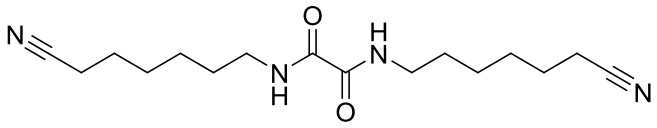

2a

N,N-bis(6-cyanohexyl)oxalamide (2a): 7-Aminoheptanenitrile (2.650 g, 21.0 mmol) was dissolved in 30 mL of THF in an argon-flushed flask. Diethyl oxalate (1.534 g, 10.5 mmol) was then added to the solution. The reaction solvent was removed *in vacuo* after 12 h. The resulting white solid was then recrystallized from ethanol. After recrystallization, the solid was subjected to reduced pressure for 30 minutes to ensure the complete removal of ethanol. The resulting white solid (4.500 g, 14.7 mmol) was obtained in 70% yield: ^{1}H NMR (300 MHz, $CDCl_3$) δ 7.47 (s,2H), 3.32 (t, *J* = 6.9 Hz, 4H), 2.35 (t, *J* = 7.0 Hz, 4H), 1.75 – 1.29 (m, 16H).[43]

Procedure for preparing PIDA cocrystals: Host **2a** (0.020 g, 0.065 mmol) and diiodobutadiyne **1** (0.040 g, 0.13 mmol) were dissolved in 3 mL acetonitrile to give a solution with a guest concentration of 13 mg/mL.. The crystallization dish was completely wrapped in foil. The foil covering the opening of the dish was punctured with a syringe needle to allow slow evaporation of solvent. Cocrystals were left to grow at room temperature. Blue cocrystals were observed after 1 day, and these crystals turned gold within 2 –3 days. Cocrystal yields were generally between 60 – 80%. The experiment was scaled appropriately for large scale

cocrystallizations. A 12 cm diameter crystallization dish was used to prepare cocrystals from 12 mL solution of host **2a**/monomer **1** in acetonitrile with a concentration of 13 mg/mL.

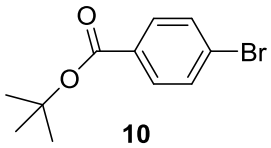

10

t-butyl-bromobenzoic acid (10): 0.3 g (1.49 mmol) of bromobenzoic acid was dissolved in 250 mL of CH_2Cl_2. t-Butyl acetate (1. 74 g, 15.87 mmol) was added into the reaction mixture followed by two drops of triflic acid was added. The reaction mixture was stirred at room temperatue for 2 h, then 100 mL of water followed by 2 M of KOH were added to quench the reaction. Products were extracted by ethyl acetate 2 x 100 mL, and solvents were removed *in vacuo*. t-Butyl bromobenzoic acid (0.15 g, 0.58 mmol) was obtained as a colorless oil in 40% yield. ^{13}C NMR (400 Mz, $CDCl_3$): δ 165.38, 132.03, 131.06, 131.50, 128, 81.84, 28.74 ppm.[55]

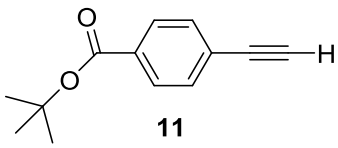

11

tert-butyl 4-ethynylbenzoate (11): A mixture of *t*-butyl 4-bromobenzoate (0.131 g, 0.6 mmol), ethynyltrimethylsilane (0.1 g, 1 mmol), dichlorobis(triphenylphosphine)palladium (2 mg, 15 μmol), triphenylphosphine (2.5 mg, 6 μmol) and copper (I) iodide (2 mg, 10 μmol) in Et_3N (3 mL) was stirred under nitrogen atmosphere under reflux for 16 h. After cooling to room temperature, the mixture was diluted with 20 mL CH_2Cl_2 and then washed with water (2×20 mL). The organic layer was dried with $MgSO_4$ and evaporated under reduced pressure to dryness. The light brown oil was dissolved in 6 mL MeOH, and 0.03 g K_2CO_3 was added. The mixture was allowed to stir at room temperature for 1.5 h. Then the reaction was worked up by removal of some MeOH by rotary evaporation, dilution with water, extraction with ether (4×20

mL), drying with MgSO4, and removal of solvent. *t*-Butyl 4-ethynylbenzoate was obtained as a brown solid (90%). ^{13}C-NMR (100MHz, $CDCl_3$) δ= 165.42, 132.29, 129.80, 129.67, 129.56, 83.36, 81.76, 80.09, 28.54 ppm.[55]

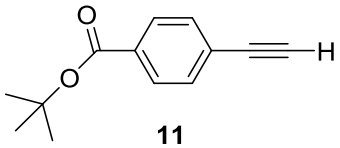

11

Attempted synthesis: tert-butyl 4-ethynylbenzoate (11): A mixture of 4-iodobenzoic acid tert-butyl ester (0.18 g, 2.02 mmol), ethynyltrimethylsilane (0.3 g, 3.3 mmol), dichlorobis(triphenylphosphine)palladium (4 mg, 30 μmol), triphenylphosphine (5 mg,12 μmol) and copper (I) iodide (4 mg, 20 μmol) in Et_3N (8 mL) was stirred under nitrogen atmosphere under reflux for 24 h. After cooling to room temperature, the mixture was washed with water (2×40 mL) and then extracted with EtOAc (2 x 40 mL). The organic layer was dried with $MgSO_4$ and evaporated under reduced pressure to dryness. The light brown oil was dissolved in 10 mL MeOH, and 0.04 g K_2CO_3 was added. The mixture was allowed to stir at room temperature for 2 h. Then the reaction was worked up by removal of some MeOH by rotary evaporation, dilution with water, extraction with EtOAc (4×20 mL), drying with $MgSO_4$. Only starting material was obtained.

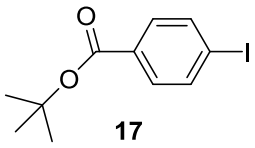

17

Attempted synthesis: 4-Iodobenzoic acid tert-butyl ester (17): A catalytic amount of DMF was added to a solution of **16** (100 mg, 0.40 mmol) and oxalyl chloride (0.12 mL, 0.65 mmol) in dry CH_2Cl_2 (10 mL). The reaction mixture was stirred at RT for 2 h and then concentrated under vacuum. The residue was dissolved in dry CH_2Cl_2 (10 mL) then t-butyl alcohol (0.38 mL, 4.03

mmol). The reaction mixture was stirred at room temperature for 4 h. The solvent was subject to rotary evaporation and a crude ^{13}CNMR (400 MHz) showed only starting material.

References

1. Field, J. E., The mechanical and strength properties of diamond. *Rep. Prog. Phys.* **2012,** *75* (12), 126505.
2. (a) Walker, J., Optical absorption and luminescence in diamond. *Rep. Pro.. Phy.* **1979,** *42* (10), 1605; (b) Wei, L.; Kuo, P. K.; Thomas, R. L.; Anthony, T. R.; Banholzer, W. F., Thermal conductivity of isotopically modified single crystal diamond. *Phys. Rev. Lett.* **1993,** *70* (24), 3764-3767.
3. Novoselov, K. S.; Geim, A. K.; Morozov, S. V.; Jiang, D.; Zhang, Y.; Dubonos, S. V.; Grigorieva, I. V.; Firsov, A. A., Electric field effect in atomically thin carbon films. *Science (New York, N.Y.)* **2004,** *306* (5696), 666-669.
4. Kaur, N.; Singh, M.; Pathak, D.; Wagner, T.; Nunzi, J. M., Organic materials for photovoltaic applications: Review and mechanism. *Synth. Met.* **2014,** *190* (0), 20-26.
5. Meng, J.; Liang, X.; Chen, X.; Zhao, Y., Biological characterizations of [Gd@C82(OH)22]n nanoparticles as fullerene derivatives for cancer therapy. *Int. Bio.* **2013,** *5* (1), 43-47.
6. Lai, Y. Y.; Cheng, Y. J.; Hsu, C. S., Applications of functional fullerene materials in polymer solar cells. *Energy. Env. Sci.* **2014,** *7* (6), 1866-1883.
7. Heeger, A. J., Semiconducting polymers: the Third Generation. *Chem. Soc. Rev.* **2010,** *39* (7), 2354-2371.
8. Scharber, M. C.; Sariciftci, N. S., Efficiency of bulk-heterojunction organic solar cells. *Prog. Polym. Sci.* **2013,** *38* (12), 1929-1940.
9. De Volder, M. F. L.; Tawfick, S. H.; Baughman, R. H.; Hart, A. J., Carbon Nanotubes: Present and Future Commercial Applications. *Science* **2013,** *339* (6119), 535-539.
10. Yu, J.-G.; Zhao, X.-H.; Yang, H.; Chen, X.-H.; Yang, Q.; Yu, L.-Y.; Jiang, J.-H.; Chen, X.-Q., Aqueous adsorption and removal of organic contaminants by carbon nanotubes. *Sci. Total Environ.* **2014,** *482–483* (0), 241-251.
11. Ai, L.; Jiang, J., Removal of methylene blue from aqueous solution with self-assembled cylindrical graphene–carbon nanotube hybrid. *Chem. Eng. J.* **2012,** *192* (0), 156-163.
12. Wang, Q.; Yan, J.; Xiao, Y.; Wei, T.; Fan, Z.; Zhang, M.; Jing, X., Interconnected porous and nitrogen-doped carbon network for supercapacitors with high rate capability and energy density. *Electrochim. Acta* **2013,** *114* (0), 165-172.
13. Choi, H. J.; Jung, S. M.; Seo, J. M.; Chang, D. W.; Dai, L. M.; Baek, J. B., Graphene for energy conversion and storage in fuel cells and supercapacitors. *Nano Energy* **2012,** *1* (4), 534-551.
14. Chen, P.; Xiao, T.-Y.; Qian, Y.-H.; Li, S.-S.; Yu, S.-H., A Nitrogen-Doped Graphene/Carbon Nanotube Nanocomposite with Synergistically Enhanced Electrochemical Activity. *Adv. Mater.* **2013,** *25* (23), 3192-3196.
15. Klapötke, T. M.; Sproll, S. M., Investigation of nitrogen-rich energetic polymers based on alkylbridged bis-(1-methyl-tetrazolylhydrazines). *J. Polym. Sci., Part A: Polym. Chem.* **2010,** *48* (1), 122-127.
16. Singh, R. P.; Verma, R. D.; Meshri, D. T.; Shreeve, J. n. M., Energetic Nitrogen-Rich Salts and Ionic Liquids. *Angew. Chem. Int. Ed.* **2006,** *45* (22), 3584-3601.
17. Eaton, P. E.; Gilardi, R. L.; Zhang, M. X., Polynitrocubanes: Advanced High-Density, High-Energy Materials. *Advanced Materials* **2000,** *12* (15), 1143-1148.

18. Chavez, D. E.; Hiskey, M. A.; Gilardi, R. D., 3,3′-Azobis(6-amino-1,2,4,5-tetrazine): A Novel High-Nitrogen Energetic Material. *Angew. Chem.* **2000,** *112* (10), 1861-1863.
19. Li, Y.-C.; Qi, C.; Li, S.-H.; Zhang, H.-J.; Sun, C.-H.; Yu, Y.-Z.; Pang, S.-P., 1,1′-Azobis-1,2,3-triazole: A High-Nitrogen Compound with Stable N8 Structure and Photochromism. *J. Am. Chem. Soc.* **2010,** *132* (35), 12172-12173.
20. Liu, A. Y.; Cohen, M. L., Structural properties and electronic structure of low-compressibility materials: β-Si3N4 and hypothetical β-C3N4. *Physical Review B* **1990,** *41* (15), 10727-10734.
21. Cohen, M. L., Calculation of bulk moduli of diamond and zinc-blende solids. *Physical Review B* **1985,** *32* (12), 7988-7991.
22. Kroke, E.; Schwarz, M., Novel group 14 nitrides. *Coord. Chem. Rev.* **2004,** *248* (5–6), 493-532.
23. Montigaud, H.; Tanguy, B.; Demazeau, G.; Alves, I.; Courjault, S., C3N4: Dream or reality? Solvothermal synthesis as macroscopic samples of the C3N4 graphitic form. *J. Mater. Sci.* **2000,** *35* (10), 2547-2552.
24. Semencha, A. V.; Pozdnyakov, O. F.; Pozdnyakov, A. O.; Blinov, L. N., Investigation of the structure of carbon-nitrogen compounds. *Glass Phys. Chem* **2008,** *34* (1), 103-109.
25. Fahmy, Y.; Shen, T. D.; Tucker, D. A.; Spontak, R. L.; Koch, C. C., Possible evidence for the stabilization of β–carbon nitride by high-energy ball milling. *J. Mater. Res.* **1999,** *14* (06), 2488-2499.
26. Gillan, E. G., Synthesis of Nitrogen-Rich Carbon Nitride Networks from an Energetic Molecular Azide Precursor. *Chem. Mater.* **2000,** *12* (12), 3906-3912.
27. Algara-Siller, G.; Severin, N.; Chong, S. Y.; Björkman, T.; Palgrave, R. G.; Laybourn, A.; Antonietti, M.; Khimyak, Y. Z.; Krasheninnikov, A. V.; Rabe, J. P.; Kaiser, U.; Cooper, A. I.; Thomas, A.; Bojdys, M. J., Triazine-Based, Graphitic Carbon Nitride: a Two-Dimensional Semiconductor. *Angew. Chem.* **2014**,126, 1-6 .
28. Fahsi, K.; Dutremez, S. G.; Vioux, A.; Viau, L., Azole-functionalized diacetylenes as precursors for nitrogen-doped graphitic carbon materials. *J. Mater. Chem.* **2013,** *1* (14), 4451-4461.
29. Jelinek, R.; Ritenberg, M., Polydiacetylenes - recent molecular advances and applications. *RSC Advances* **2013,** *3* (44), 21192-21201.
30. Carpick, R. W.; Sasaki, D. Y.; Marcus, M. S.; Eriksson, M. A.; Burns, A. R., Polydiacetylene films: a review of recent investigations into chromogenic transitions and nanomechanical properties. *J. Phys.: Condens. Matter* **2004,** *16* (23), R679.
31. Yarimaga, O.; Jaworski, J.; Yoon, B.; Kim, J.-M., Polydiacetylenes: supramolecular smart materials with a structural hierarchy for sensing, imaging and display applications. *Chem. Commun.* **2012,** *48* (19), 2469-2485.
32. Lee, J.-S.; Lee, S.; Kim, J.-M., Fluorogenic conjugated polymer fibers from amphiphilic diacetylene supramolecules. *Macromolecular Research* **2008,** *16* (1), 73-75.
33. Yoon, B.; Ham, D.-Y.; Yarimaga, O.; An, H.; Lee, C. W.; Kim, J.-M., Inkjet Printing of Conjugated Polymer Precursors on Paper Substrates for Colorimetric Sensing and Flexible Electrothermochromic Display. *Adv. Mater.* **2011,** *23* (46), 5492-5497.
34. Kootery, K. P.; Jiang, H.; Kolusheva, S.; Vinod, T. P.; Ritenberg, M.; Zeiri, L.; Volinsky, R.; Malferrari, D.; Galletti, P.; Tagliavini, E.; Jelinek, R., Poly(methyl methacrylate)-Supported Polydiacetylene Films: Unique Chromatic Transitions and Molecular Sensing. *Appl. Mater. Inter.* **2014,** *6* (11), 8613-8620.

35. Sun, A.; Lauher, J. W.; Goroff, N. S., Preparation of Poly(diiododiacetylene), an Ordered Conjugated Polymer of Carbon and Iodine. *Science* **2006,** *312* (5776), 1030-1034.
36. (a) Baughman, R. H., Solid-State Synthesis of Large Polymer Single-Crystals. *J. Poly. Sci.- Part B-Poly. Phys.* **1974,** *12* (8), 1511-1535; (b) Wegner, G., Topochemical Reactions of Monomers with Conjugated Triple Bonds .I. Polymerization of 2.4-Hexadiyn-1.6-Diols Derivatives in Crystalline State. *Zeitschrift Fur Naturforschung Part B-Chemie Biochemie Biophysik Biologie Und Verwandten Gebiete* **1969,** *B 24* (7), 824-&.
37. Lauher, J. W.; Fowler, F. W.; Goroff, N. S., Single-Crystal-to-Single-Crystal Topochemical Polymerizations by Design. *Acc. Chem. Res.* **2008,** *41* (9), 1215-1229.
38. Goroff, N. S.; Curtis, S. M.; Webb, J. A.; Fowler, F. W.; Lauher, J. W., Designed cocrystals based on the pyridine-iodoalkyne halogen bond. *Org. Lett.* **2005,** *7* (10), 1891-1893.
39. Chernick, E. T.; Tykwinski, R. R., Carbon-rich nanostructures: the conversion of acetylenes into materials. *J. Phys. Org. Chem.* **2013,** *26* (9), 742-749.
40. Chalifoux, W. A.; Tykwinski, R. R., Synthesis of polyynes to model the sp-carbon allotrope carbyne. *Nature Chemistry* **2010,** *2* (11), 967-971.
41. Luo, L.; Resch, D.; Wilhelm, C.; Young, C. N.; Halada, G. P.; Gambino, R. J.; Grey, C. P.; Goroff, N. S., Room-Temperature Carbonization of Poly(diiododiacetylene) by Reaction with Lewis Bases. *J. Am. Chem. Soc.* **2011,** *133* (48), 19274-19277.
42. Yevsyukov, S. Y.; Kudryavtsev, Y. P.; Korshak, Y. V.; Khvostov, V. V.; Babaev, V. G.; Guseva, M. B.; Korshak, V. V., Synthesis of Carbyne on the Basis of Polyvinylidene Halides. *Vysokomolekulyarnye Soedineniya Seriya A* **1989,** *31* (1), 27-33.
43. Resch, D., Poly(diiododiacetylene): A Potential Precursor for New All-Carbon Materials. Stony Brook University, Stony Brook, NY, 2013.
44. (a) Wilhelm, C.; Boyd, S. A.; Chawda, S.; Fowler, F. W.; Goroff, N. S.; Halada, G. P.; Grey, C. P.; Lauher, J. W.; Luo, L.; Martin, C. D.; Parise, J. B.; Tarabrella, C.; Webb, J. A., Pressure-Induced Polymerization of Diiodobutadiyne in Assembled Cocrystals. *J. Am. Chem. Soc.* **2008,** *130* (13), 4415-4420; (b) Sougawa, M.; Sumiya, T.; Takarabe, K.; Mori, Y.; Okada, T.; Gotou, H.; Yagi, T.; Yamazaki, D.; Tomioka, N.; Katsura, T.; Kariyazaki, H.; Sueoka, K.; Kunitsugu, S., Bond strengths of New Carbon-nitride-Related material C 2 N 2 (CH 2). *J. Phys.* **2012,** *377* (1), 012028.
45. Hofmanbang, N., The Iiodine-Azide Reaction .1. The Catalytic Effect of the Tetrathionate Ion. *Acta Chem. Scand.* **1949,** *3* (7), 872-885.
46. (a) Kurzawa, J.; Janowicz, K., Use of a stopped-flow technique for investigation and determination of thiourea and its N-methyl derivatives as inducers of the iodine–azide reaction. *Anal. Bioanalytical. Chem.* **2005,** *382* (7), 1584-1589; (b) Zakrzewski, R., Development and validation of a reversed-phase HPLC method with post-column iodine-azide reaction for the determination of thioguanine. *J. Anal. Chem.* **2009,** *64* (12), 1235-1241.
47. (a) Ferrari, A. C.; Rodil, S. E.; Robertson, J., Interpretation of infrared and Raman spectra of amorphous carbon nitrides. *Phys. Rev. B:Condens. Matter.* **2003,** *67* (15), 155306; (b) Yap, Yoke K.; Kida, S.; Aoyama, T.; Mori, Y.; Sasaki, T., High-Temperature Synthesis of Amorphous Carbon Nitride Thin Films with Modified Microstructure. *Jpn. J. Appl. Phys.* **1998,** *37* (6B), L746.
48. Luo, L.; Wilhelm, C.; Sun, A.; Grey, C. P.; Lauher, J. W.; Goroff, N. S., Poly(diiododiacetylene): Preparation, Isolation, and Full Characterization of a Very Simple Poly(diacetylene). *J. Am. Chem. Soc.* **2008,** *130* (24), 7702-7709.

49. Luo, L.; Wilhelm, C.; Young, C. N.; Grey, C. P.; Halada, G. P.; Xiao, K.; Ivanov, I. N.; Howe, J. Y.; Geohegan, D. B.; Goroff, N. S., Characterization and Carbonization of Highly Oriented Poly(diiododiacetylene) Nanofibers. *Macromolecules* **2011,** *44* (8), 2626-2631.
50. Kormachev, V. V.; Mitrasov, Y. N., Unsaturated Phosphorylated Aldehydes and their Reactions with Alkylidenephosphoranes. *Zh. Obshch. Khim.* **1975,** *45* (6), 1270-1273.
51. Vasil'eva, E. I.; Freidlina, R. K., Amination of 1-cyano-6-chlorohexane, the telomerization product of ethylene, by means of cyanogen chloride. *Izv. Akad. Nauk SSSR, Ser. Khim.* **1964,** (Copyright (C) 2014 American Chemical Society (ACS). All Rights Reserved.), 1233-6.
52. Duan, C.; Huang, F.; Cao, Y., Recent development of push-pull conjugated polymers for bulk-heterojunction photovoltaics: rational design and fine tailoring of molecular structures. *J. Mater. Chem.* **2012,** *22* (21), 10416-10434.
53. Price, S. C.; Stuart, A. C.; Yang, L. Q.; Zhou, H. X.; You, W., Fluorine Substituted Conjugated Polymer of Medium Band Gap Yields 7% Efficiency in Polymer-Fullerene Solar Cells. *J. Am. Chem. Soc.* **2011,** *133* (12), 4625-4631.
54. Xu, R.; Schweizer, W. B.; Frauenrath, H., Perfluorophenyl–Phenyl Interactions in the Crystallization and Topochemical Polymerization of Triacetylene Monomers. *Chem. Eur. J.* **2009,** *15* (36), 9105-9116.
55. Ang, X., Synthesis, Co-crystallization and Polymerization of Novel Push-Pull Diynes & Attempts toward Ordered Polymerization of Diiodooctatetrayne. Stony Brook University, Stony Brook, NY., Unpublished.
56. Sonogashira, K., Development of Pd–Cu catalyzed cross-coupling of terminal acetylenes with sp2-carbon halides. *J. Organomet. Chem.* **2002,** *653* (1–2), 46-49.
57. Christensen, H.; Schjøth-Eskesen, C.; Jensen, M.; Sinning, S.; Jensen, H. H., Synthesis of 3,7-Disubstituted Imipramines by Palladium-Catalysed Amination/Cyclisation and Evaluation of Their Inhibition of Monoamine Transporters. *Chem. Eur. J.* **2011,** *17* (38), 10618-10627.